Electronic Supplementary Material (ESI) for Nanoscale.

In vivo Deep-Tissue Microscopy with UCNP/Janus-Dendrimers as Imaging Probes: Resolution at Depth and Feasibility of Ratiometric Sensing

Supporting Information

Shane Plunkett,[1] Mirna El Khatib,[1] İkbal Şencan,[2] Jason E. Porter,[2] Anand T. N. Kumar,[2] Joshua E. Collins,[3] Sava Sakadžić[2] and Sergei A. Vinogradov[1]*

[1] Department of Biochemistry and Biophysics, Perelman School of Medicine, and Department of Chemistry, School of Arts and Sciences, University of Pennsylvania, Philadelphia, PA 19104

[2] Athinoula A. Martinos Center for Biomedical Imaging, Massachusetts General Hospital/Harvard Medical School, Charlestown, MA 02129

[3] Intelligent Materials Solutions, Inc., Princeton, NJ 08540

E-mail: vinograd.upenn@gmail.com

Table of Contents

1. Synthesis

Scheme S1. Dendrons used in this study.

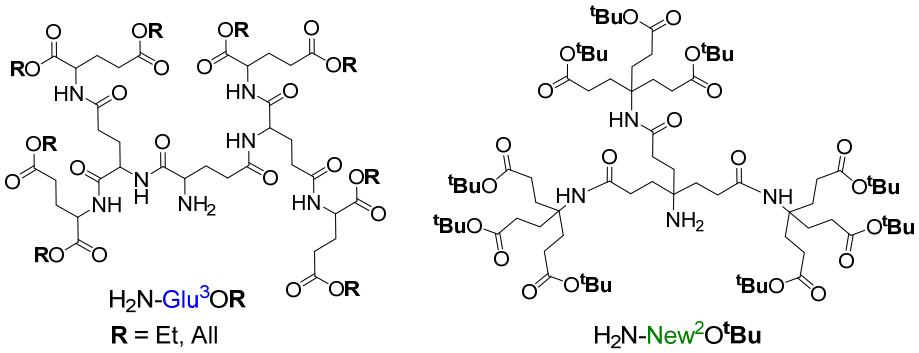

Scheme S2. Synthesis of the a*llyl*-terminated polyglutamic dendrons.

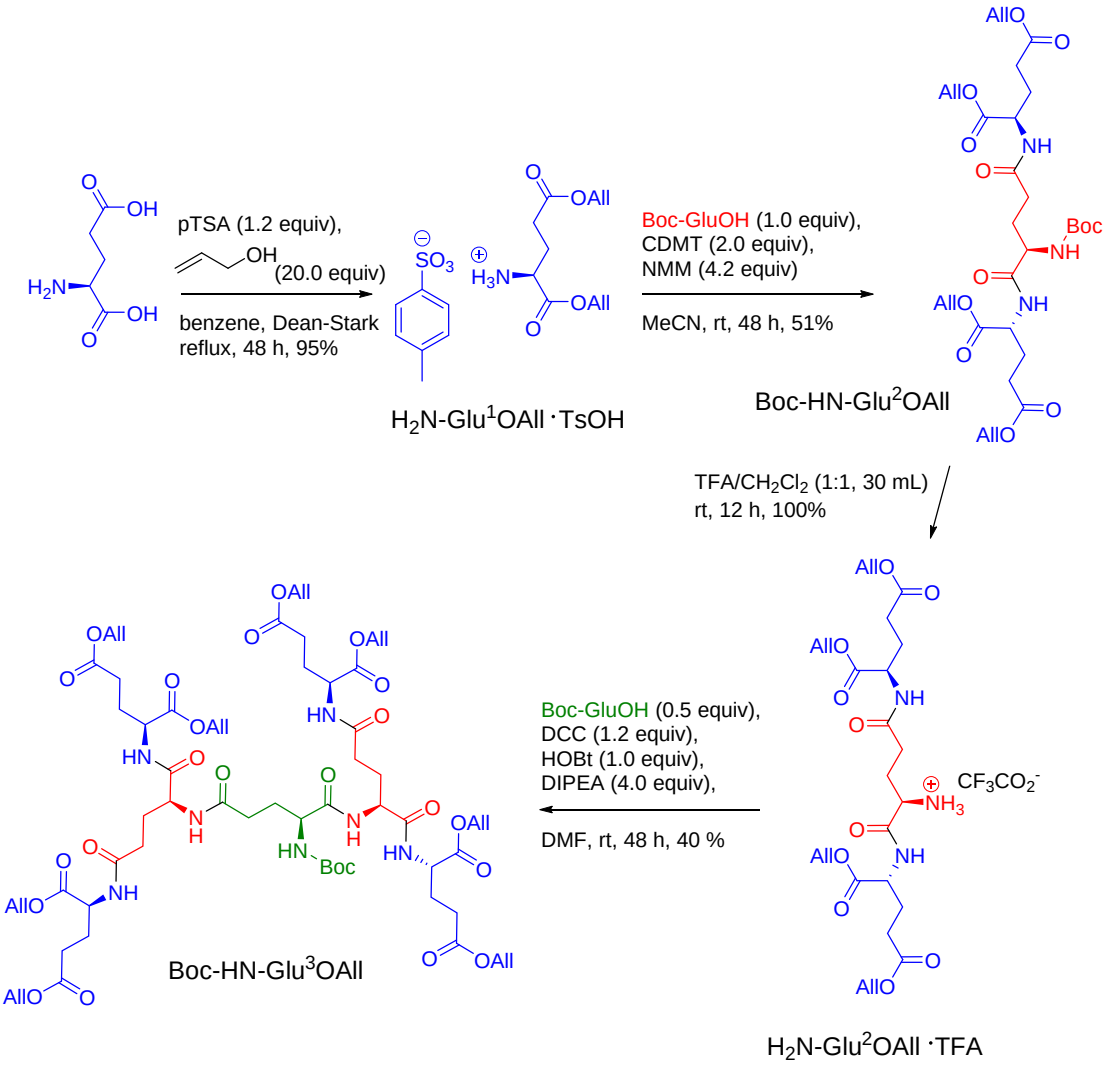

H_2N-Glu^1-OAll·TsOH

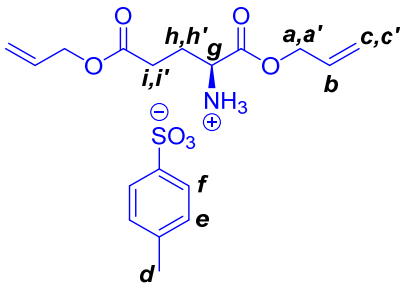

L-Glutamic acid (30.0 g, 0.20 mol), *p*-toluenesulfonic acid (TSA; 46.5 g, 0.24 mol, 1.2 equiv), allyl alcohol (272 mL, 4.00 mol, 20 equiv) were refluxed in benzene (300 mL) for 48 h in a flask (1L), equipped with a Dean-Stark trap and a refluxing condenser. The water formed during the reaction was collected in the trap and removed. The mixture was allowed to cool to room temperature, and the solvent was removed under reduced pressure. Et_2O (~30 mL) was added to the resulting yellow-orange oil, and the mixture was left overnight at room temperature. The precipitate formed was collected by filtration under suction, washed with cold Et_2O and dried under vacuum to afford the product as a beige salt (76.9 g, 0.19 mol, 95%). ^{1}H NMR (500 MHz, $CDCl_3$) δ = 8.40 (brs, 3H, *NH*), 7.48 (d, J = 8.1 Hz, 2H, ***f***), 7.11 (d, J = 7.8 Hz, 2H, ***e***), 5.96 – 5.85 (m, 2H, ***b***), 5.41-5.15 (m, 4H, ***c,c'***), 4.72-4.60 (m, 2H, ***a'***), 4.57-4.51 (m, 2H, ***a***), 4.15-4.05 (m, 1H, ***g***), 2.61-2.47 (m, 2H, ***h,h'***), 2.28 (s, 3H, ***d***), 2.16-1.95 ppm (m, 2H, ***i,i'***); ^{13}C NMR (126 MHz, DMSO-d_6) δ = 171.3, 168.8, 145.3, 137.9, 132.6, 131.7, 128.1, 125.5, 118.8, 117.9, 66.1, 64.7, 51.3, 28.9, 25.2 and 20.8 ppm; MALDI-TOF (m/z): $[M+Na]^+$ calcd for $C_{18}H_{25}NO_7SNa$, 422.13; found 423.48.

Boc-HN-Glu^{2}OAll

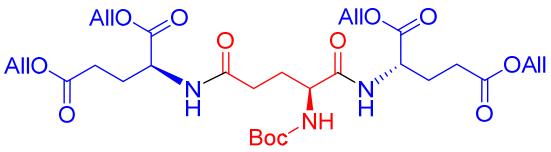

A mixture of *N*-(tert-butoxycarbonyl)-L-glutamic acid (Boc-GluOH) (9.38 g, 0.038 mol) in acetonitrile (300 mL) was cooled to 0°C on an ice bath under stirring in a round-bottom flask (1L). 4,6-Dimethoxy-1,3,5-triazine (CDMT) (13.34 g, 0.076 mol, 2.0 equiv) was added to the mixture, followed by addition of N-methylmorpholine (NMM) (8.50 mL, 0.076 mol, 2.1 equiv). The mixture was stirred for 2h, H_2N-Glu^{1}OAll·TsOH (30.31 g, 0.076 mol, 1.0 equiv) and NMM (8.50 mL, 0.076 mol, 2.1 equiv) were added, and stirring continued for 48 h at r.t. The resulting yellow solution was concentrated under reduced

pressure, H_2O (300 mL), slightly acidified by HCl (3 drops of conc. solution), was added, leading to formation of a white precipitate, and the mixture was stirred overnight at r.t. The solid was collected by centrifugation, washed with aq. HCl (0.1N) and dried under vacuum to afford the target compound as a beige solid (26.02 g, 0.039 mol, 51%). ^{1}H NMR (500 MHz, DMSO-d_6) δ = 8.39-8.25 (m, 2H), 6.95 (d, J = 6.9 Hz, 1H), 6.05-5.87 (m, 4H), 5.36 (dd, J = 16.7, 10.1 Hz, 4H), 5.27 (d, J = 9.5 Hz, 4H), 4.71-4.54 (m, 8H), 4.47-4.31 (m, 2H), 4.06-3.94 (s, 1H), 2.66-2.38 (m, 5H), 2.33-2.20 (m, 2H), 2.16-2.04 (m, 2H), 1.96-1.89 (m, 2H), 1.82-1.65 (m, 1H), 1.44 ppm (s, 9H); ^{13}C NMR (126 MHz, DMSO-d_6) δ 172.2, 172.0, 171.9, 171.8, 171.5, 171.2, 155.3, 132.6, 132.4, 132.3, 117.9, 117.8, 117.7, 117.6, 78.1, 65.0, 64.9, 64.5, 64.5, 53.8, 51.2, 51.1, 31.6, 29.8, 29.6, 28.2, 27.8 and 26.1 ppm; MALDI-TOF (m/z): $[M+Na]^+$ calcd for $C_{32}H_{47}N_3O_{12}Na$, 688.306; found 688.037; $[M+K]^+$ calcd for $C_{32}H_{47}N_3O_{12}K$, 704.28; found 704.47.

Boc-HN-Glu^{3}OAll

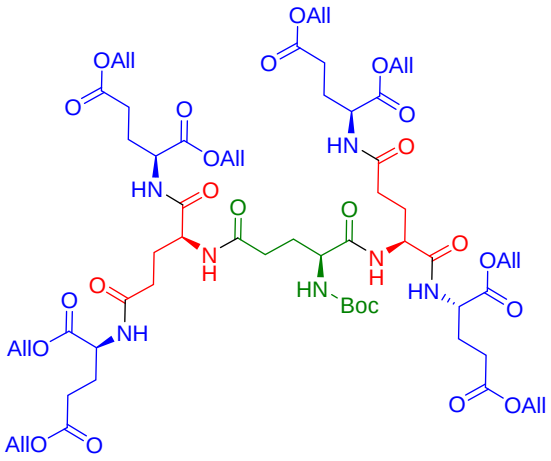

Step 1: In a round-bottom flask (200 mL), Boc-HN-Glu^{2}OAll (7.13 g, 0.01 mol) was dissolved in dichloromethane (DCM, 10 mL). The solution was cooled to 0°C on an ice bath and trifluoroacetic acid (TFA) (20 mL) was added. The mixture was stirred overnight at rt. The completion of the reaction was verified by MALDI-TOF analysis, after which the solvents (DCM and TFA) were removed under reduced pressure. DCM was added and re-evaporated, and this cycle was repeated three times. Thus obtained material, H_2N-Glu^{2}OAll·TFA, was used in the following reaction without purification.

Step 2: H_2N-Glu^{2}OAll·TFA, obtained as described above, was dissolved in DMF (20 mL). Hydroxybenzotriazole (HOBt) (1.45 g, 10.7 mmol, 1.0 equiv) and then *N,N*-diisopropylethylamine (DIPEA) (7.70 mL, 42.8 mmol, 4.0 equiv) were added to the mixture under continuous stirring. The resulting solution was transferred portion-wise to another round-bottom flask (500 mL), in which Boc-

GluOH (2.65 g, 10.7 mmol) and *N,N'*-dicyclohexylcarbodiimide (DCC) (2.65 g, 12.84 mmol, 1.2 equiv) had been stirred in DMF (100 mL) for 1h at r.t. under Ar atmosphere. The resulting mixture was allowed to react at r.t. for 48h under stirring. The solvent was removed under reduced pressure, and the remaining viscous solid was dissolved in EtOAc (200 mL). The solution was washed with HCl (1.0N; 3×100 mL), $NaHCO_3$ (aq. saturated; 2×100 mL), HCl (1.0N; 100 mL), brine (200 mL), dried over anhydr. Na_2SO_4, filtered, and the solvents were evaporated under reduced pressure to afford Boc-HN-Glu^{3}OAll as a light yellow solid (2.87 g, 2.14 mmol, 40 %). ^{1}H NMR (500 MHz, DMSO-d_6) δ = 8.47-8.35 (m, 1H), 8.34-8.16 (m, 2H), 8.06-7.85 (m, 2H), 5.94-5.82 (m, 8H), 5.27 (dd, J = 17.2, 10.9 Hz, 8H), 5.21-5.12 (m, 8H), 4.61-4.53 (m, 8H), 4.53-4.45 (m, 8H), 4.33-4.26 (m, 4H), 2.48-2.35 (m, 7H), 2.24-2.13 (m, 6H), 2.08-1.95 (m, 5H), 1.93-1.80 (m, 7H), 1.76-1.64 (m, 3H), 1.35 ppm (s, 9H). ^{13}C NMR (126 MHz, DMSO-d_6) δ = 174.1, 173.7, 173.2, 172.1, 172.0, 171.9, 171.6, 171.6, 171.5, 171.3, 171.2, 168.6, 168.3, 168.1, 168.0, 167.8, 162.0, 157.2, 150.0, 132.7, 132.4, 132.3, 118.1, 118.0, 117.7, 78.3, 65.1, 65.0, 64.6, 64.2, 55.5, 55.2, 55.1, 54.3, 54.2, 53.7, 53.3, 51.9, 51.3, 48.7, 43.6, 31.6, 31.4, 30.0, 29.9, 28.2, 27.5, 26.1 and 26.1 ppm; MALDI-TOF (m/z): $[M+Na]^+$ calcd for $C_{64}H_{91}N_7O_{24}Na$, 1364.601; found 1364.993.

Scheme S3. Synthesis of Janus dendrimers **4** and **9**.

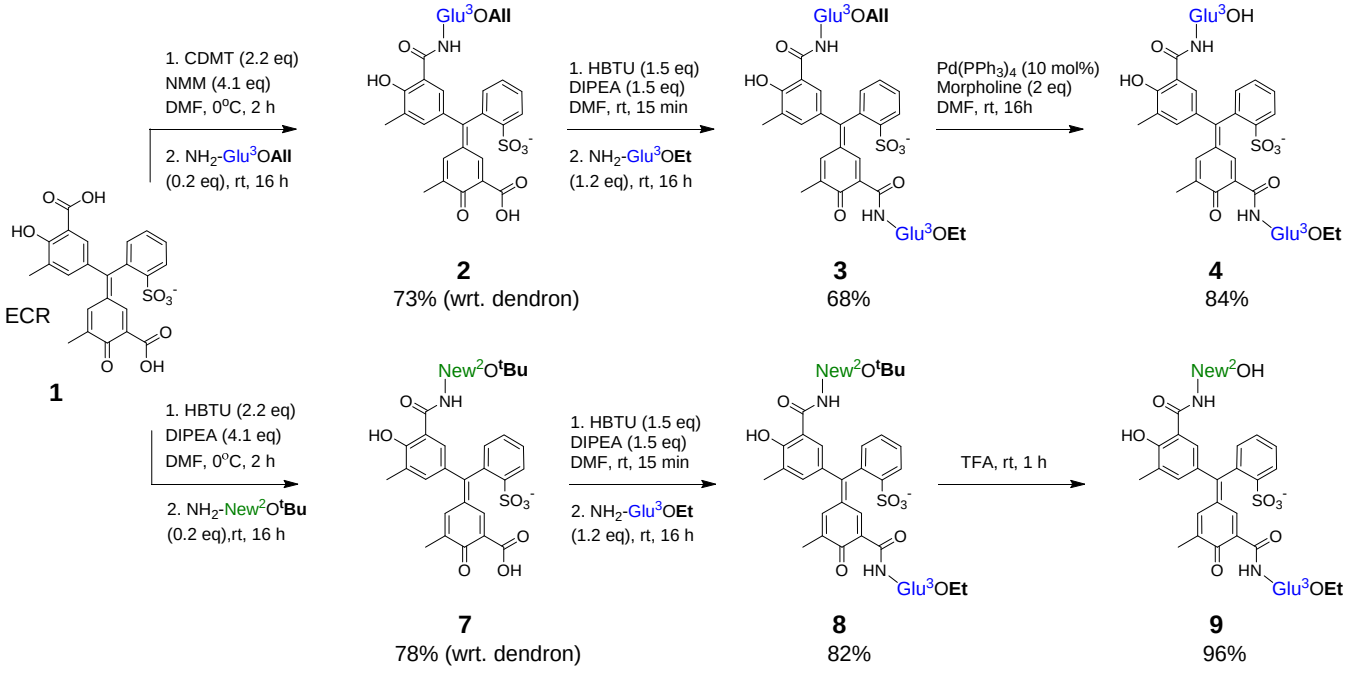

Scheme S4. Synthesis of PEGylated dendrimers **6a-c** and **11**.

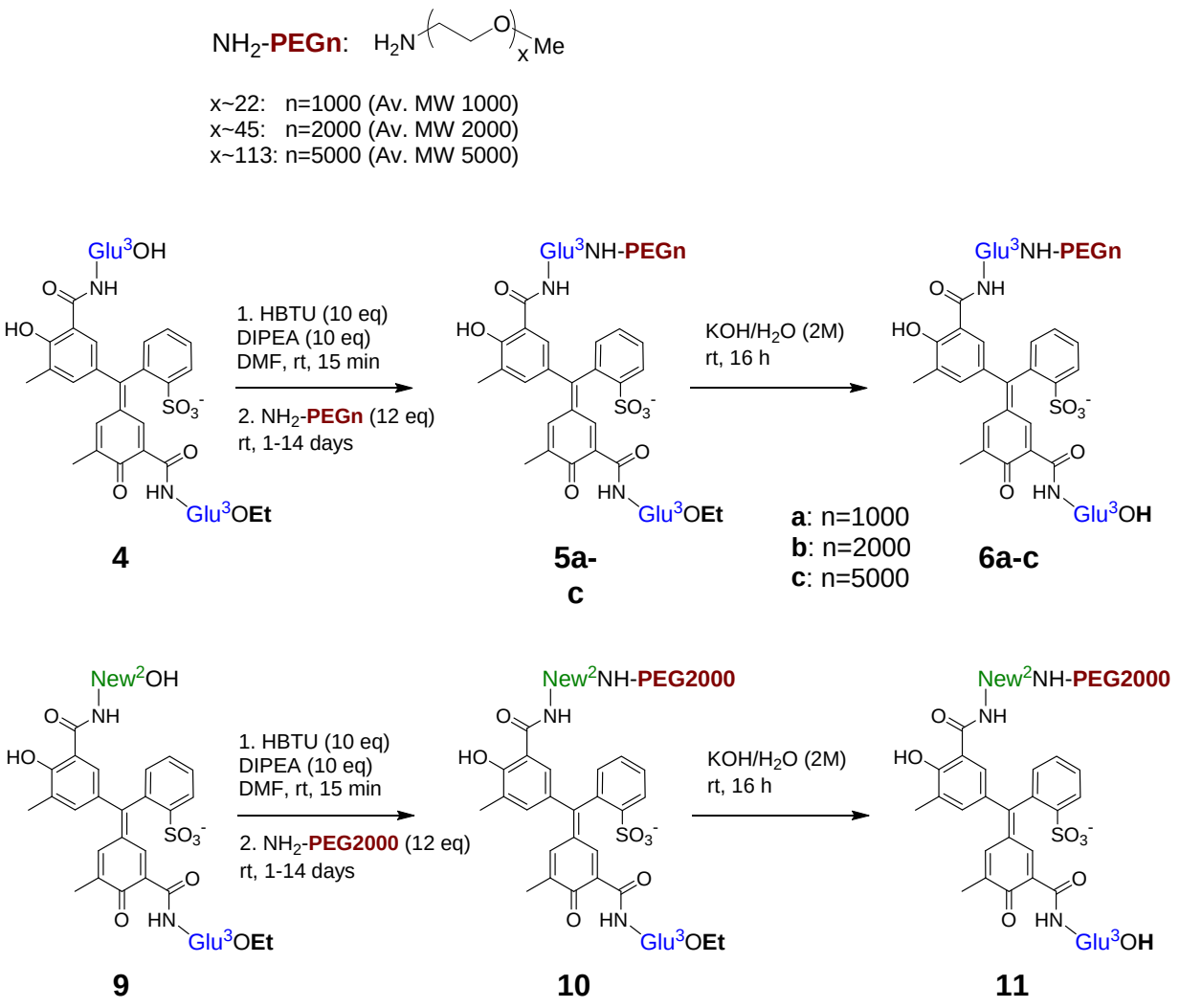

General description of the synthesis:

The dendrons were assembled by the convergent method[1, 2] as described earlier,[3] using Boc-protected glutamic acid as a building block and CDMT and/or HBTU-mediated coupling reactions (Scheme S2). The deprotection of the focal group in these syntheses requires application of acid (e.g. TFA), and hence the peripheral carboxylic esters have to be able to sustain acidic conditions. We used allyl and ethyl esters on dendrimer faces intended for PEGylation and for binding to UCNPs, respectively. Allyl-terminated dendrons were more difficult to isolate, since they showed a tendency towards aggregation, forming viscous residues upon removal of solvent. Nevertheless, multigram quantities of the dendrons

up to Gen 3, Boc-HN-Glu^{3}OEt and Boc-HN-Glu^{3}OAll, were successfully prepared. These compounds are stable and can be stored in bulk for subsequent use.

mono-Amidation of the *bi*-carboxylic ECR core (**1**), which is readily available, could be carried out simply using an excess of **1**, taking advantage of the large size of the Gen 3 dendron. Once attached to ECR, the dendritic branch impeded addition of the second dendron, minimizing formation of the symmetric product (Scheme 1). Small amounts of the latter could be efficiently removed by size-exclusion chromatography (SEC), and pure *mono*-dendronized ECR (**2**) was isolated in 70-75% yield.

Addition of the second dendron to **2** yielded the target Janus system **3**. In this case, an excess of the reactant (dendron) was used to facilitate coupling, since the remaining free carboxylic acid anchor point on **3** was shielded by the already attached branch. Curiously, the order in which the dendrons, allyl *vs* ethyl, were attached to **1** proved crucial for the overall yield. When the ethyl-terminated dendron was coupled first, the subsequent attachment of the allyl counterpart was completely unsuccessful: no target dendrimer could be detected in the reaction mixture by mass-spectrometry. But when the order was switched, i.e. allyl- and then ethyl-, the dendrimer formed in good yield. This unusual behavior may be related to aggregation of the allyl dendrons in solution.

The issues presented in the synthesis of the allyl dendrons led us to investigate other dendritic systems. For example, commercial Gen 2 Newkome-type dendrons,[4] which are available as *t*Bu esters, have similar number of peripheral carboxylates as Gen 3 glutamate and do not suffer from aggregation. The corresponding Janus-dendrimer **8** was built in the same manner as compound **3**, and both compounds were used in subsequent reactions.

Our previous work on dendritically protected oxygen probes[5, 6] has shown that modification with polyethylene glycols (PEG) can be efficient for converting even extremely hydrophobic dendrimers into completely water-soluble inert macromolecules. At the same time, PEGylation is known, at least in some cases, to reduce the rate of systemic clearance. Based on these considerations, our Janus dendritic ligands were designed to possess a PEG-interface for aqueous solubilization. PEGylation of the

dendrimers was carried out using monomethoxy-PEG-amines,[7] ensuring that the resulting linkages can sustain base-mediated hydrolysis as well as action of non-specific esterases *in vivo*.

Removal of the more labile protecting group, i.e. allyl or *t*Bu in dendrimers **3** and **8**, generated molecules **4** and **9**, respectively, having free carboxyl groups, which were introduced into the subsequent amidation reactions with monomethoxy-PEG-amines (Av. MW 1000, 2000 and 5000). UV/Vis absorption measurements confirmed that complete PEGylaton was achievable, but required longer reaction times as the PEG size increased. Finally, removal of the ethyl ester groups by basic hydrolysis gave the target dendrimers **6** and **11**.

(ECR)-HN-Glu^{3}OAll (**2**). In a round-bottom flask (200 mL), Eriochrome Cyanine R (ECR) **1** (590 mg, 1.10 mmol, 5.0 equiv) was dissolved in DMF (30 mL) under stirring, and the mixture was cooled to 0°C on an ice bath. CDMT (425 mg, 2.42 mmol, 11.1 equiv) was added to the mixture together with NMM (0.5 mL, 4.5 mmol, 20.4 equiv), and it was allowed to react for 3h. In a separate flask, Boc-HN-Glu^{3}OAll (300 mg, 0.22 mmol, 1.0 equiv) was treated with neat TFA (10 mL) in CH_2Cl_2 (10 mL) for 2h at r.t. The solvents were removed under reduced pressure, after which CH_2Cl_2 (20 mL) was added and evaporated from the residue three times to ensure removal of acid. The residue was dissolved in DMF (10 mL), and the remaining traces of TFA were quenched by NMM. The resulting solution was added to the first mixture, and the combined solution was stirred at r.t. for 48 h, after which the solvent was removed under reduced pressure. The resulting residue was taken up in DCM (100 mL) and washed sequentially with HCl aq. (0.1N; 2×100 mL), water (100 mL) and brine (100 mL). The organic phase was collected, dried over anhydr. Na_2SO_4, and the solvents were removed under reduced pressure. The remaining residue was dissolved in THF (5-10 mL) and filtered through cotton wool. The product was purified by size-exclusion chromatography (SEC) using THF as eluent. The target compound was isolated as the second colored band, which was re-purified in the same manner. After removal of solvents, the material was precipitated upon addition of Et_2O and sonication. It was isolated by centrifugation and dried in vacuum to yield the title compound as a purple solid (271 mg, 0.16 mmol, 73 %). ^{1}H NMR (400 MHz, DMSO-d_6) δ = 8.36-7.86 (m, 10H), 7.47-6.92 (m, 7H), 5.86-5.81 (m, 8H), 5.28-5.22 (m, 8H), 5.16 (d, J = 11.2 Hz, 8H), 4.61-4.53 (m, 8H), 4.52-4.50 (m, 8H), 4.24-4.20 (m, 6H), 2.50 (br s, 3H), 2.38 (br s, 7H), 2.33-2.29 (m, 3H), 2.19-2.10 (m, 6H), 2.06-1.79 (m, 12H), 1.74-1.60 ppm (m, 3H). ^{13}C NMR (101 MHz, DMSO-d_6) δ = 174.4, 172.9, 175.5, 172.4, 133.7, 133.5, 133.4,

133.3, 129.1, 128.8, 119.1, 118.8, 66.1, 66.0, 65.9, 65.8, 65.6, 65.4, 57.1, 55.8, 55.3, 52.3, 49.9, 30.9, 27.0. 19.9. 19.8, 19.7, 16.3, and 12.4 ppm; MALDI-TOF (m/z): $[M+H]^+$ calcd for $C_{82}H_{99}N_7O_{30}S$, 1693.616; found 1693.650.

EtOGlu^3-NH-(ECR)-HN-Glu^{3}OAll (3). **2** (220 mg, 130 μmol, 1.0 equiv) was dissolved in DMF (15 mL), HBTU (60 mg, 156 μmol, 1.2 equiv) was added to the solution together with DIPEA (0.1 mL, excess), and the mixture was allowed to react for 15 min at r.t. H_2N-Glu^{3}OEt (178 mg, 156 μmol, 1.2 equiv) was added to the solution in one portion, and the resultant mixture was stirred at r.t. for 72h. The solvent was removed under reduced pressure, and the resulting residue was dissolved in THF (5-10 mL) and filtered through cotton wool. The product was purified by size-exclusion chromatography (SEC) using THF as eluent. The target compound was isolated as the second colored band, and after concentrating the material was re-purified in the same manner. After removal of solvents, the final material was precipitated upon addition of Et_2O and sonication. The title compound was isolated by centrifugation, dried in vacuum and isolated as a purple solid (248 mg, 88 μmol, 68 %). ^{1}H NMR (500 MHz, DMSO-d_6) δ = 8.66-7.79 (m, 17H), 7.46-6.53 (m, 7H), 5.87 (br s, 8H), 5.29-5.26 (m, 8H), 5.18-5.16 (m, 8H), 4.51 (br s, 16H), 4.26-4.21 (m, 9H), 4.06-4.02 (m, 16H), 2.96-2.71 (m, 8H), 2.53 (br s, 3H), 2.40-2.34 (m, 16H), 2.16-2.15 (m, 10H), 2.00-1.95 (m, 11H), 1.82-1.80 (m, 12H), 1.70-1.66 (m, 3H), 1.17-1.13 ppm (m, 24H). ^{13}C NMR (101 MHz, DMSO-d_6) δ = 174.4, 173.3, 173.2, 172.9, 172.9, 172.8, 172.5, 168.7, 133.7, 133.5, 133.4, 130.0, 129.7, 129.1, 129.0, 118.9, 118.8, 70.9, 66.0, 65.9, 65.6, 61.8, 61.7, 61.6, 61.0, 57.1, 55.2, 53.1, 52.4, 52.3, 47.4, 32.6, 31.0, 30.9, 29.0, 27.1, 27.0, 19.9, 19.7, 16.3, 15.2, 15.1 and 15.0 ppm; MALDI-TOF (m/z): $[M+H]^+$ calcd for $C_{133}H_{182}N_{14}O_{51}S$, 2823.179; found 2823.274.

EtOGlu^3-NH-(ECR)-HN-Glu^{3}OH·(4). **3** (50 mg, 18 μmol, 1 equiv) was dissolved in DMF (5 mL), $Pd(PPh_3)_4$ (18 mg, 16 μmol, 0.9 equiv) and morpholine (0.14 mL, 1.6 mmol, 9.0 equiv) were added, and the mixture was stirred for 18 h at r.t. After removal of solvents, THF (20 mL) was added to the reaction flask, and the suspension was sonicated for 10 min. Isolation of the title compound was achieved by centrifugation. The residue was washed with THF and then twice with Et_2O. The residual solvents were removed upon drying under high vacuum overnight. The title compound was isolated as an octa-morpholine complex as a dark purple solid (38 mg, 15 μmol, 84 %). ^{1}H NMR (500 MHz, DMSO-d_6) δ = 8.21-7.88 (m, 5H), 7.60-6.94 (m, 13H), 5.87 (br s, 8H), 4.20 (br s, 7H), 4.03 (br s, 16H), 3.80-3.36 (m, 46H) 2.98-2.71 (m, 32H), 2.33-2.17 (m, 24H), 1.94-1.74 (m, 33H), 1.14 ppm (br s, 24H). ^{13}C NMR (101 MHz, DMSO-d_6) δ = 173.4, 173.2, 172.9, 172.9, 172.8, 172.7, 172.6, 172.5, 172.4, 172.3, 162.2, 162.1,

134.3, 133.3, 133.2, 133.1, 132.6, 132.5, 129.9, 129.8, 128.2, 70.9, 68.1, 67.8, 67.3, 66.9, 66.8, 65.1, 61.8, 61.7, 61.6, 61.0, 57.1, 55.3, 55.2, 52.3, 46.2, 44.4, 30.9, 30.8, 27.1, 27.0, 26.2, 19.7, 15.2, 15.1 and 15.0 ppm.

(ECR)-HN-Newk^{2}O^{t}Bu (7). **1** (590 mg, 1.10 mmol, 5.0 equiv) was dissolved in DMF (50 mL) together with HBTU (917 mg, 2.42 mmol, 11.0 equiv) and DIPEA (0.5 mL, 4.5 mmol, 20.5 equiv), and the mixture was allowed to react for 15 min at r.t. NH_2-Newk^{2}O^{t}Bu (317 mg, 0.22 mmol, 1.0 equiv)[8] was added in one portion and the resultant solution was stirred at r.t. for 48 h, after which DMF was removed by rotary evaporation. The resulting residue was taken up in CH_2Cl_2 (100 mL) and washed sequentially with aq. HCl (0.1N), water and brine. The organic phase was dried over anhydr. Na_2SO_4, and solvents were completely removed under reduced pressure. The residue was dissolved in THF (15 mL) and passed through cotton wool. The product was purified by size-exclusion chromatography (SEC) using THF as eluent. The target compound was isolated as the second colored band, which, after concentrating, was re-purified in the same manner. After removal of solvents, the final material was precipitated upon addition of hexanes and sonication. The target compound was isolated by centrifugation, dried in vacuum and isolated as a purple solid (325 mg, 0.17 mmol, 78 %). ^{1}H NMR (500 MHz, DMSO-d_6) δ = 8.37-8.05 (m, 2H), 7.99 (d, J = 7.5 Hz, 1H), 7.73-7.19 (m, 7H), 7.07-6.75 (m, 2H), 2.17-2.00 (m, 30H), 1.84-1.71 (m, 24H), 1.37 ppm (s, 81H). ^{13}C NMR (101 MHz, DMSO-d_6) δ = 173.3, 173.0, 80.6, 57.5, 54.7, 42.9, 30.2, 29.9, 28.8, 19.9, 19.2, 17.8 and 13.6 ppm; MALDI-TOF (m/z): $[M+H]^+$ calcd for $C_{99}H_{152}N_4O_{29}S$, 1893.026; found 1893.148.

EtOGlu^3-NH-(ECR)-HN-Newk^{2}O^{t}Bu (8). The title compound was prepared following the same procedure as described for **3**, but staring from **7** (200 mg, 106 µmol, 1.0 equiv), using HBTU (45 mg, 116 µmol, 1.2 equiv), DIPEA (0.1 mL, excess) and NH_2-Glu^{3}OEt (133 mg, 116 µmol, 1.2 equiv).[9] The title compound was precipitated upon sonication in hexanes, collected by centrifugation, dried in vacuum and isolated as a purple solid (262 mg, 87 µmol, 82 %). ^{1}H NMR (500 MHz, DMSO-d_6) δ = 8.66-8.50 (m, 2H), 8.39-8.12 (m, 6H), 7.89-7.54 (m, 4H), 7.45-7.24 (m, 7H), 7.10-6.69 (m, 2H), 4.29-4.21 (m, 6H), 4.05-4.02 (m, 16H), 2.96 (br s, 3H), 2.80 (br s, 2H), 2.52 (s, 3H), 2.35-2.34 (m, 8H), 2.16-2.15 (m, 7H), 2.05-2.03 (m, 24H), 1.98-1.95 (m, 12H), 1.81-1.75 (m, 28H), 1.35 (s, 81H), 1.17-1.14 ppm (m, 24H). ^{13}C NMR (101 MHz, DMSO-d_6) δ = 173.4, 173.3, 273.2, 173.1, 173.0, 172.9, 172.8, 272.7, 172.6, 172.5, 172.4, 172.3, 171.5, 162.2, 128.9, 108.1, 80.6, 61.8, 61.8, 61.7, 61.6, 61.5, 61.1, 61.0, 57.5, 53.2, 52.6, 52.4, 52.3, 47.4, 31.0, 30.9, 30.8, 30.2, 30.0, 28.8, 27.1, 19.9, 15.2, 15.1, and 15.0 ppm; MALDI-TOF (m/z): $[M+H]^+$ calcd for $C_{150}H_{234}N_{11}O_{50}S$, 3021.582; found 3021.849.

EtOGlu^3-NH-(ECR)-HN-Newk^{2}OH (9). **8** (30 mg, 10 μmol, 1 equiv) was dissolved in neat trifluoroacetic acid (10 mL) and stirred at r.t. for 3 h. The solvents were removed fully by rotary evaporation, and the resulting residue was washed three times with CH_2Cl_2 (20 mL) to remove residual traces of acid. The compound was dried overnight under high vacuum and isolated as a bright red solid (24 mg, 9.6 μmol, 96 %). ^{1}H NMR (500 MHz, DMSO-d_6) δ = 12.02 (s, 9H), 8.66-8.03 (m, 7H), 7.88-7.74 (m, 3H), 7.64-7.25 (m, 9H), 7.08-6.76 (m, 2H), 4.26-4.21 (m, 6H), 4.06-3.96 (m, 16H), 2.96 (br s, 3H), 2.80 (br s, 2H), 2.52 (s, 3H), 2.34 (br s, 8H), 2.16-2.15 (m, 8H), 2.08 (br s, 24H), 1.97-1.95 (m, 11H), 1.79 (br s, 31H), 1.15-1.14 ppm (m, 24H). ^{13}C NMR (101 MHz, DMSO-d_6) δ = 175.5, 173.2, 173.0, 172.9, 172.8, 162.2, 129.0, 128.9, 66.0, 61.8, 61.7, 61.6, 61.5, 61.1, 61.0, 57.4, 53.2, 52.3, 47.4, 35.5, 32.2, 31.3, 30.9, 30.8, 30.1, 29.2, 27.1, 27.0, 19.9, 16.3, 15.2, 15.1 and 15.0 ppm.

Synthesis of compounds 5a-c and 10 - general PEGylation procedure. In a typical procedure, a sample of the precursor dendrimer, **4** or **9** (~10 mg, 1.0 equiv), was dissolved in DMF (30 mL) together with HBTU (10.0 equiv) and DIPEA (>10.0 equiv). After 15 min the appropriate NH_2-PEGn (10.0 equiv) was added, and the reaction left to stir at r.t. After 48 h another portion of HBTU (10.0 equiv) and NH_2-PEGn (3-4 equiv) was added. Upon reaction completion, the solvents were completely removed by rotary evaporation, and the residue was taken up in THF (10 mL). The solution was filtered through cotton, and the product was isolated by SEC. Typically, SEC was performed twice on each sample. The PEGylated dendrimer eluted as the first colored band. The solvent was removed by rotary evaporation, and the product was dried overnight under high vacuum.

The effectiveness of PEGylation was evaluated by measuring the absorbance of a solution of the target material of known concentration (by weight) in an aq. buffer (phosphate, 10 mM, pH 8), assuming that the molar extinction coefficient of the PEGylated dendrimer e.g. at the peak absorption of ECR core was the same as that of the ECR itself (~40,000 $M^{-1}cm^{-1}$). The time required for a reaction to complete generally increased with increase in the weight of NH_2-PEGn. Reactions with PEG1000 were typically complete within 48-72 h, while reactions with PEG2000 took 4-5 days, and completion of reactions with PEG5000 required 10-14 days. Whenever PEGylation had not gone to completion, the reaction was restarted.

Synthesis of compounds 6a-c and 11. In a typical procedure, a sample of **5a-c** or **10** (~100-300 mg) was dissolved in MeOH (10 mL) and KOH (~1 g) was added, upon which the solution turned dark purple due to complete deprotonation of the ECR core. After stirring for 2 h, the reaction mixture was

diluted with water (100 mL) and left to stir for additional 16 h. The resulting solution was acidified with HCl conc. to pH~2, and the mixture was stirred for 10 min. The pH was adjusted to ~7, and the dendrimer was purified by dialysis against deionised water (membrane cut-off 12,000-14,000 Da) for 3-5 days. The purified solution was lyophilized to give the target compound (**6a-c** or **11**) as a red solid in a near quantitative yield.

Modification of UCNPs with dendritic ligands. In a typical procedure,[10] a sample of an organic ligand (**6a-c** or **11**) was dissolved in a mixture of water and DMF (~2:3 v/v) to give a ligand concentration of ~10 mg/mL. A solution of UCNPs pre-treated with $NOBF_4$ in DMSO or DMF (~50 mg/mL) was added to the resulting mixture, so that the ratio (by mass) of UCNP:ligand was ~1:2. The mixture was stirred for 1 h at r.t. and poured into distilled water (40 mL per 100 mg of UCNP). The UCNP-dendrimers were isolated *via* centrifugation (8,000 g, 15-30 min). After centrifugation the precipitated gel was separated from the supernatant, and the latter was re-centrifuged again until no further precipitation was observed. The centrifuge speed was kept such that the acceleration was below 10,000 g. To remove the excess of the ligand and residual organic solvents, the obtained gel-like precipitates were combined, re-dispersed in distilled water, and the target UCNP-dendrimers was precipitated again by centrifugation. This procedure was repeated several times, after which the gel was re-dissolved in distilled water to a final concentration of ~2.5 mg/mL for spectroscopic measurements or ~25 mg/mL for animal imaging experiments. The final solution of the UCNP/dendrimer was filtered through a syringe filter (pore size 0.4 μm).

2. Transmission Electron Microscopy (TEM)

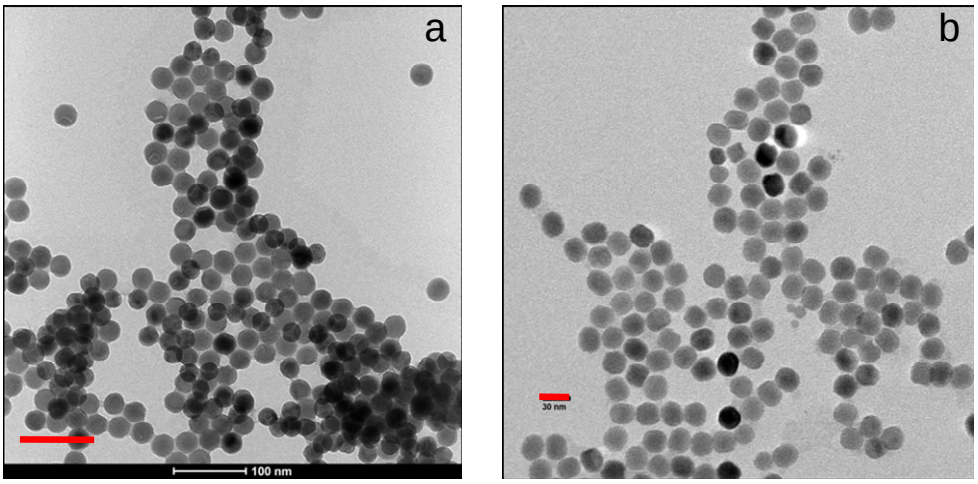

Figure S1. TEM images acquired on a JEM-1400 microscope (Jeol) using a 120 kV accelerating voltage: (a) UCNP/BF_4^- (bar: 100 nm); (b) UCNP-**6b** (bar: 30 nm).

3. Stability of UCNP/dendrimers in aqueous solutions

The stability of UCNP/dendrimers in aqueous solutions was assessed spectrophotometrically. In a typical experiment, an optical cuvette (1 cm path length) was filled with an aqueous medium containing the material of interest (salts, proteins etc.), and an aliquot of a concentrated sample of UCNP-**6b** or UCNP-**11** was added to reach the final concentration of ~1 mg/mL. The absorption spectra of the sample were recorded every 10 min for a period of ~17h (100 measurements). For particles that are insoluble or unstable in the medium, aggregation should first lead to an increase in turbidity (increase in absorbance), but after reaching certain size the aggregates should begin precipitating and thus clearing the optical path (see e.g. Fig. S3). For soluble/stable particles no changes in absorption are expected.

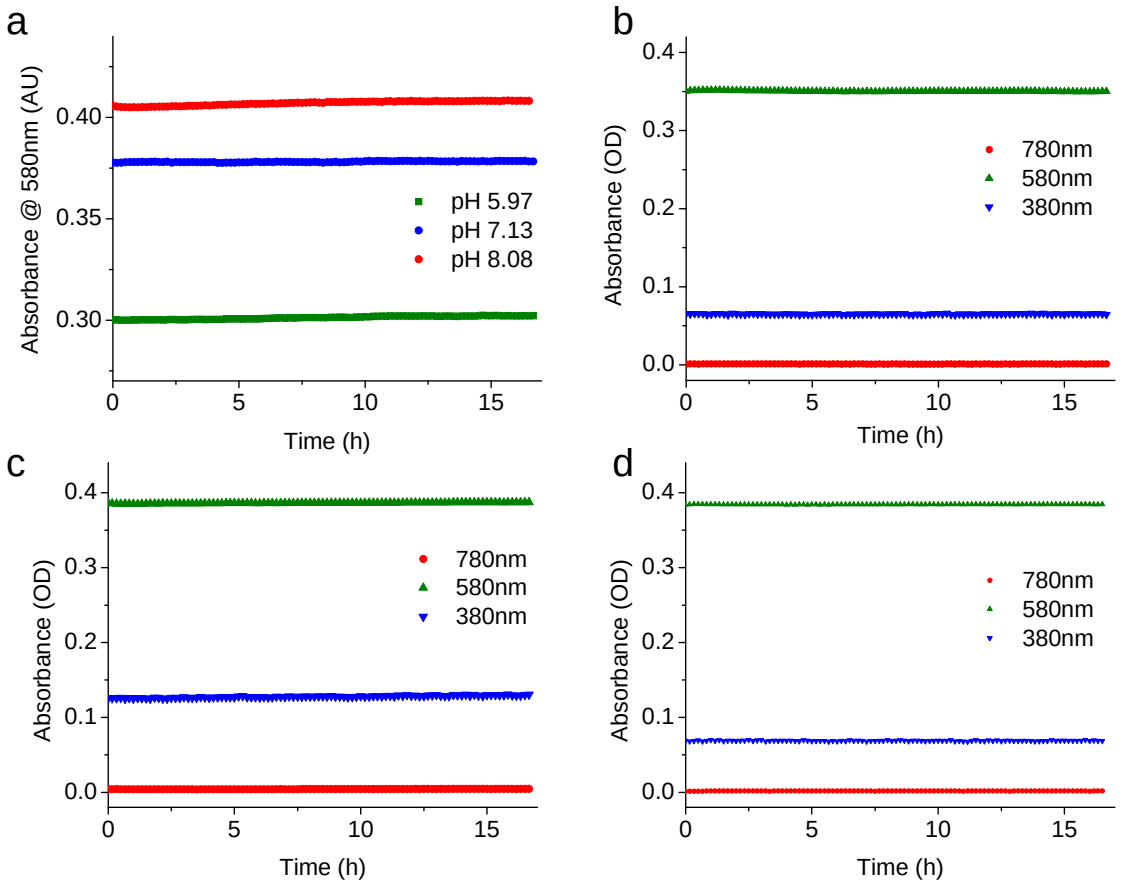

Figure S2. Spectroscopic evaluation of stability of UCNP/dendrimes in aqueous solutions. Traces in the graphs show absorbances at selected wavelengths. (a) Changes in absorbance of UCNP-**11** (λ_{abs}=580 nm) at different pH over time (~2.5 mg/mL, 50 mM HEPES). (b) Changes in the absorbance of UCNP-**6b** in the presence of $Ca(OAc)_2$ (2 mM) and NaCl (10 mM), HEPES buffer (50 mM, pH 7.13). (c) Changes in the absorbance of UCNP-**6b** in the presence of $MgCl_2$ (2 mM) and NaCl (10 mM), HEPES buffer (50 mM, pH 7.13). (d) Changes in the absorbance of UCNP-**6b** in the presence of $ZnCl_2$ (2 mM) and NaCl (10 mM), HEPES buffer (50 mM, pH 7.13).

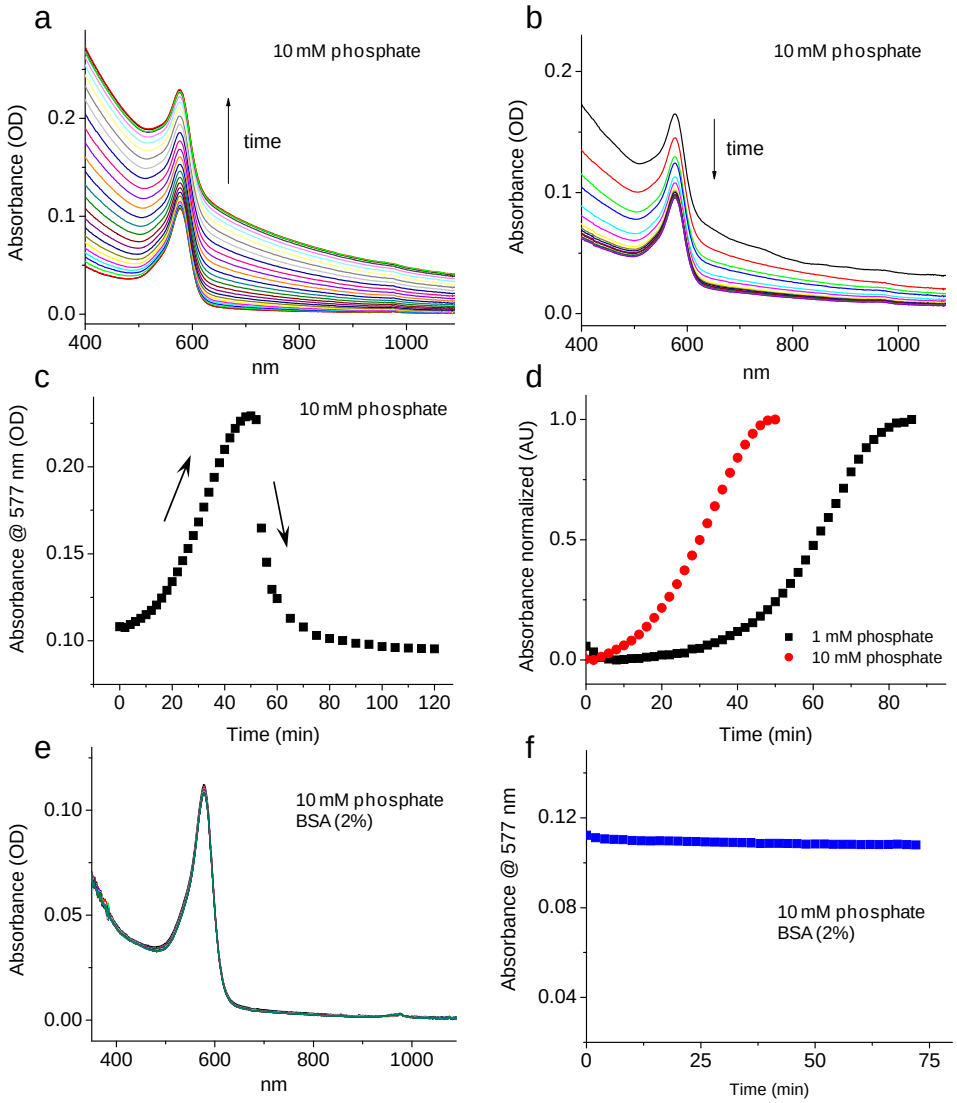

Figure S3. Changes in the absorption spectra of UCNP-**11** in the presence of phosphate. A stock solution of UCNP-**11** (30 μL, 25 mg/mL) was added to 0.5 mL of phosphate buffer (10 mM, pH 7.2). Spectra were recorded each 2 min for ~60 min, then every 5 min. (a) Initial aggregation phase: growth in the absorbance due to the rise of the scattering baseline. (b) Precipitation phase: decrease in the absorbance due to clearing of the optical path. (c) Changes in absorbance at 578 nm, showing the kinetics of both phases. (d) Kinetics of aggregation, as monitored by absorbance at 578 nm, for 10 mM and 1 mM phosphate solutions. (e) Absorption spectra of UNCP-**11** stabilized in the presence of phosphate (10 mM, pH 7.2) by bovine serum albumin (BSA, 2% by weight). (f) Changes in absorbance at 578 nm.

4. Attenuation of UCNP emission by media absorption and scattering

Note: In these experiments a different batch of UCNPs was used to generate UCNP/dendrimers. Hence, the emission spectra have slightly different shape.

Effect of unbound absorber in the medium. Aliquots of PdR4 (a Pd porphyrin-based macromolecular dye)[7] were added to a solution of UCNP-**11** in HEPES buffer (10 mM, pH 6.95). PdR4 is not expected to interact with UCNP-**11** in any way, since it is an uncharged fully PEGylated molecule.[7] Absorption and emission spectra were recorded upon each addition (Fig. S4). The emission spectra were recorded in a right-angle configuration, such that the laser beam passed through the middle of an optical cuvette (1 cm). Thus, the distance from the laser path, where the emission was excited, to the exit window, where the emitted photons exited the cuvette, was ~0.5 cm.

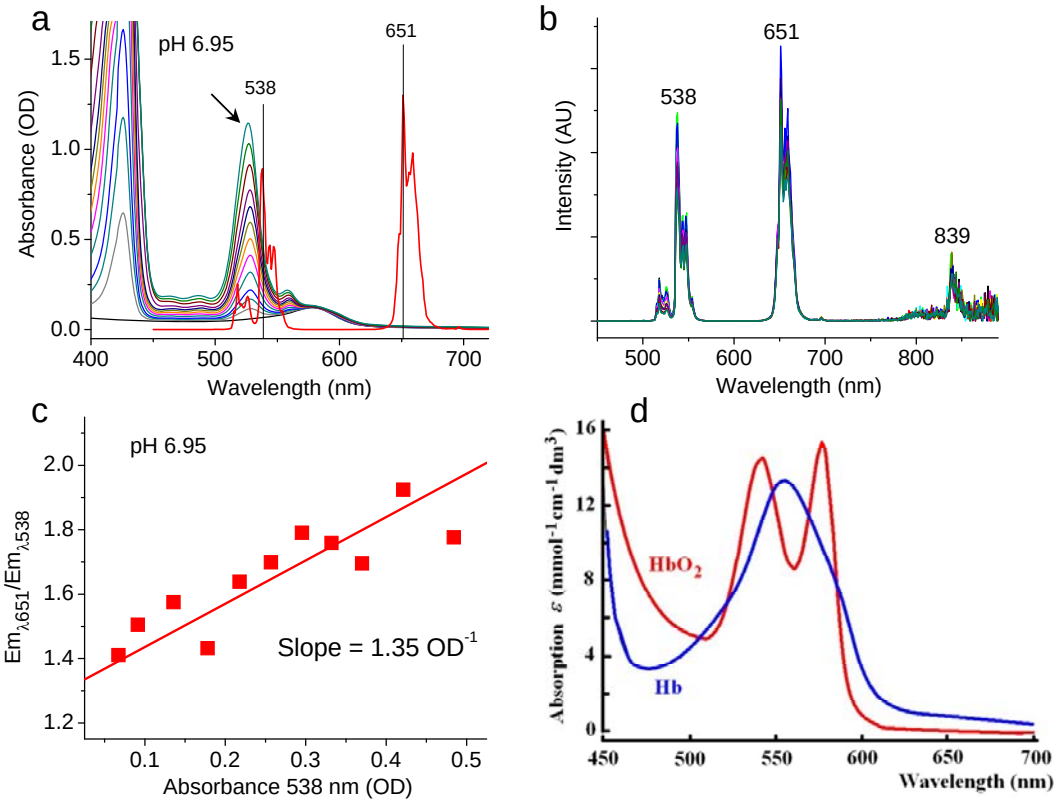

Figure S4. (a) Absorption spectra of UCNP-**11** upon addition of PdR4. An arbitrarily scaled UCNP emission spectrum is shown in red to illustrate the spectral overlap. The arrow points at the spectrum of the sample containing maximal added amount of PdR4, used in the scattering experiments (below). (b) Emission spectra (λ_{ex}=980 nm) of the samples whose absorption is shown in (a). Changes in the ratios of the integrated intensities of emission of UCNP-**11** as a function of absorbance at 538 nm: (c) Em(λ_{651})/Em(λ_{538}); (d) Absorption spectra of different forms of hemoglobin.

In this optical configuration, the slope of the emission ratio $Em(\lambda_{651})/Em(\lambda_{538})$ was found to be ~1.35 OD^{-1}, while the slope of the same ratio as a function of pH was ~0.31 $(pH\ unit)^{-1}$ (see the Main Text, Fig. 2). These values indicate that a change in the medium absorbance (through the optical path separating the emitting species from the detector) of only ~0.2 OD would be needed to induce changes in the ratio $Em(\lambda_{651})/Em(\lambda_{538})$ similar to those induced by a pH change of nearly one unit (close to pH 6). *In vivo* such changes in absorbance can be easily encountered even over sub-millimeter distances. Furthermore, only a shoulder of the absorption band of PdR4 (λ_{max}=524 nm) overlaps with the main 'green' emission peak of UCNPs (λ_{max}=538 nm) (Fig. S4a), making this synthetic dye only a moderate attenuator of UCNP emission. In contrast, hemoglobin and other Fe porphyrin-containing proteins have their absorption spectra almost entirely overlapping with the 'green' Er^{3+} emission band (Fig. S4d). Therefore, their effect on the emission ratio without doubt will be much more pronounced.

Effect of scattering. Aliquots of a solution of Itralipid (Sigma) were added to the sample from the experiment above, containing maximal added amount of PdR4 (the corresponding absorption spectrum is marked with an arrow in Fig. S4a). The emission ratios were plotted as a function of the scattering offset at 850 nm (Fig. S5).

First we note a substantial increase in the emission intensity upon the initial addition of the scatterer. As the photon path length becomes longer due to the multiple scattering events, more nanoparticles interact with the incident beam and generate more of upconverted light. But the following additions lead to a decrease in the emission intensity, as more and more photons become absorbed in the layers close to the entrance of the beam into the medium, and less and less of emitted photons are able to reach the detector due to an inner-filter effect. The key conclusion from this experiment, however, is that regardless of the total emission intensity, the ratios of the bands change monotonously and pronouncedly as a function of scatterer's concentration. Indeed, scattering increases absorption by the medium due to an increase in the photon path length. Since PdR4 absorbs stronger in the green, the 'green' emission band is attenuated stronger, and the ratio $Em(\lambda_{651})/Em(\lambda_{538})$ increases.

The above experiments demonstrate that heterogeneities in absorption and scattering are able to non-negligibly affect the ratios of the UCNP emission bands. Thus, a ratiometric scheme underlying sensing of an analyte distributed through a heterogeneous medium (e.g. biological tissue) must be carefully evaluated for its ability to permit quantitative detection.

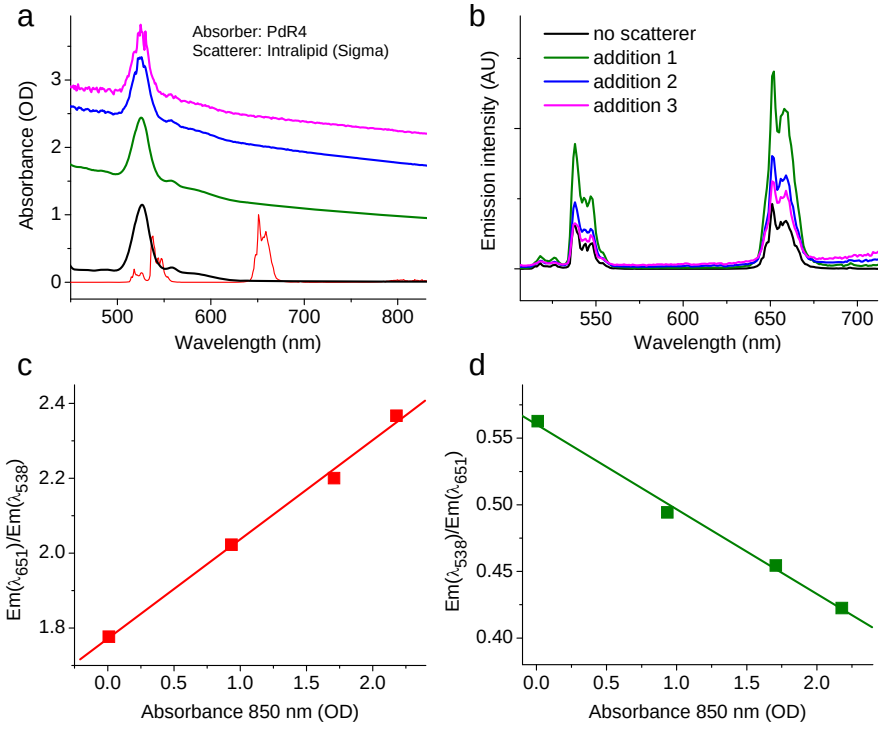

Figure S5. (a) Absorption spectra of UCNP-**11** with added PdR4 and subsequent additions of scatterer (Intralipid, Sigma). An arbitrarily scaled UCNP emission spectrum is shown in red to illustrate the spectral overlap. (b) Emission spectra (λ_{ex}=980 nm) of the samples whose absorption is shown in (a). Changes in the ratios of the integrated intensities of emission of UCNP-**11** as a function of absorbance at 850 nm: (c) $Em(\lambda_{651})/Em(\lambda_{538})$, (d) $Em(\lambda_{538})/Em(\lambda_{651})$.

5. *In vivo* animal imaging experiments

Animal preparation and maintenance. *In vivo* performance of UNCP/dendrimers was assessed by imaging cortical microvasculature in 3 months-old C57BL/6 mice (female, Charles River Laboratories). During the surgery, the mice were anesthetized using 1.5%-2% isoflurane in a mixture with air and oxygen (2% isofluorane for anesthesia induction, 1.5% during surgical procedures). Mice were tracheotomized for ventilation, and the femoral artery was cannulated to permit intravascular injection of imaging agents (UCNP/dendrimers, FITC-dextran) as well as for measurements of the blood pressure, heart rate and blood gases. The animal eyes were covered with a lubricant. The body temperature was monitored by a rectal thermometer and maintained at 37°C throughout the entire preparation and experiment using a heating blanket. The craniotomy (round shape, 3 mm in diameter) was performed over the right hemisphere, centered over the parietal bone. The dura was removed and the cranial

window was sealed with a 150-μm-thick glass coverslip using a dental acrylic. After surgery the mice were transferred to a microscopy room and placed under a microscope. During imaging anesthesia (1% isoflurane in a mixture of air and oxygen) was constantly maintained.

For imaging with UCNP/dendrimers, the blood plasma was labeled by injecting an aqueous solution of UCNP-**11** (0.15 mL, 25 mg/mL) through the cannula inserted in to the femoral artery. All surgical and experimental procedures were performed in accordance with the guidelines established by the MGH Institutional Animal Care and Use Committee (IACUC).

Imaging setup. Imaging was performed using a custom-built two-photon microscopy system (Fig. S6, left).[11, 12] Conventional fluorescent probes (e.g. FITC-dextran) were excited with a tunable femtosecond laser (Insight, Spectra-Physics, 680-1300 nm, 80 MHz rep. rate), while UCNP/dendrimers were excited with a continuous wave (CW) laser diode (Laserglow Tech, 980 nm). Power attenuation and temporal gating were performed using an electro-optic modulator (EOM) (ConOptics, 350-160). The beam was steered in the lateral plane (X&Y) by two galvanometer-mirrors (Cambridge Technologies, 6215HB). The microscope objective lens (XLUMPLFLN-W, 20x, NA=1, WD=2 mm, Olympus) was moved along the optical Z-axis using a motorized stage in order to focus excitation at the desired imaging depth. The UCNP emission was collected by the objective lens, reflected by an epi-dichroic mirror (Semrock Inc., FF875-Di01-25x36), passed through a short-pass filter (Semrock Inc., FF01-890/SP-50) and directed to a photomultiplier tube (PMT, Hamamatsu, H10770PA-50) through a bandpass filter (Semrock Inc., FF01-709/167-25). This PMT was used in photon counting mode for recording emission decays and in analog mode for fast raster scanning.

Deep microangiographic imaging. In a typical experiment, UCNP-**11** in the blood plasma was excited by a rectangular excitation gate (e.g. 20-50 μs-long), and the emission was detected by a PMT over the following 250-280 μs. In the experiment shown in Fig. 3, the field of view (FOV) was 440×440 μm^2 (250×250 pixels). Typically, at each cortical depth a 10-μm-thick stack of images was recorded, stepping over 2 μm in Z. A MIP image was computed by selecting the maximum intensity value throughout the stack. The power of the excitation beam was increased as deeper cortical layers were imaged.

Image deconvolution. The laser beam was raster-scanned across the FOV of 735×735 μm^2 (500×500 pixels) at a cortical depth of ~100 μm with the speed corresponding to the pixel dwell times of 5-40 μs. Thus obtained images were subjected to a deconvolution using the Richardson-Lucy method, as implemented in Matlab (deconvlucy(); Mathworks Inc). For each pixel dwell time *T*, the point spread function (PSF) was calculated as F(t/*T*), where F(t) is the luminescence time profile. The profile F(t) was

obtained by measuring luminescence *in vivo* in several intravascular locations (n=12) in time-resolved fashion, using the same excitation gate as in imaging. The individual profiles were averaged and normalized to give the function F(t). Prior to deconvolution the images were filtered by using a two-dimensional median filter (medfilt2, Matlab Inc) with the neighborhood size of 3×3 pixels. The mean value and standard deviation of the image background away from the vessels were used as 'deconvlucy' parameters for additive noise ('readout') and damping threshold ('dampar'), respectively.

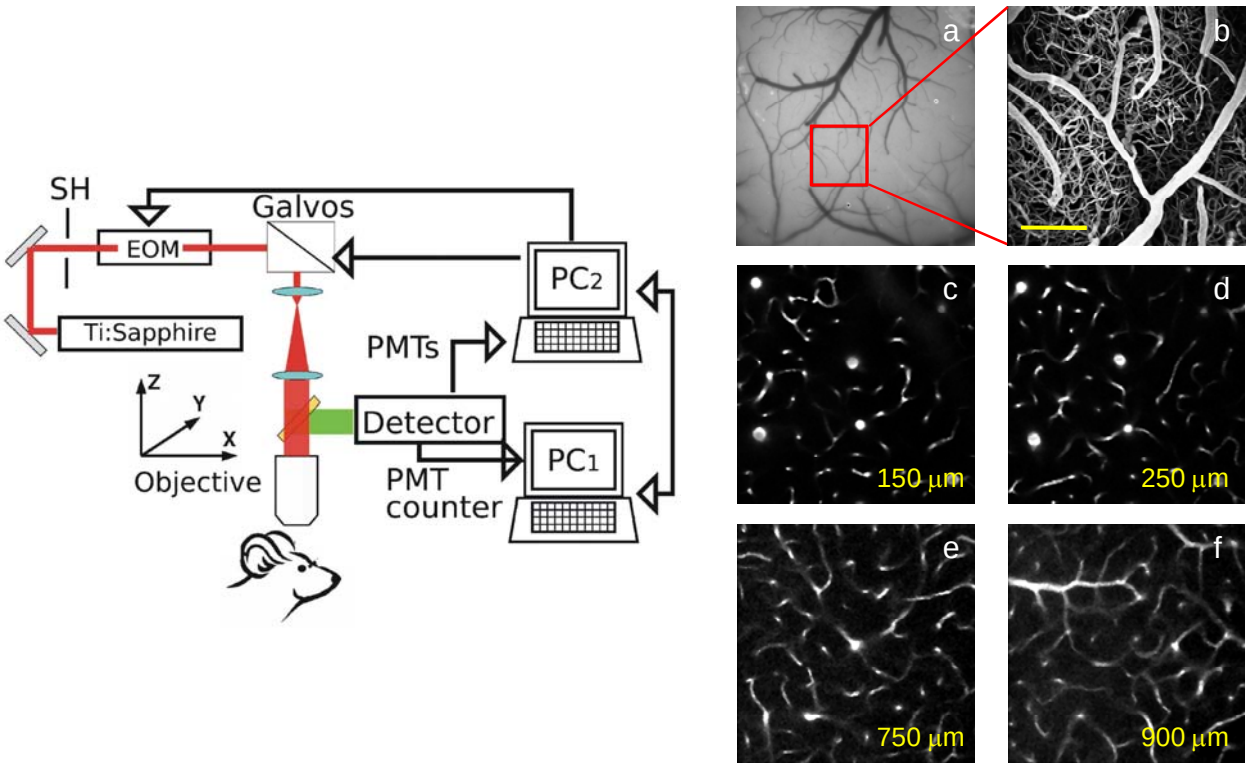

Figure S6. (Left) Schematic representation of the multiphoton microscopy setup used in this study. The system consists of a Ti:Sapphire laser, which in the case of excitation of UCNPs was replaced by a CW laser diode, an Electrooptic Modulator (EOM) for gating the laser, galvanometric mirrors for scanning the beam in X-Y plane, several detectors with the corresponding optical filters for recording signals at different wavelengths, the objective lens and several controlling computers. (Right) Images of the vasculature in live mouse brain. (a) Image of the brain surface obtained with a CCD camera upon green light illumination. The segment in red rectangle is shown in images b-f. (b) Maximum Intensity Projection (MIP) image of a stack extending from the surface to 610 μm depth, obtained using FITC as a vascular marker and two-photon excitation by a femtosecond laser: λ_{ex}=950 nm, 150 fs pulse length, 80 MHz rep. rate. Bar: 100 μm. (c-f) Images of the same segment at different scanning depths, obtained using UCNP-**11** as a marker and excitation by a CW laser (λ_{ex}=980 nm) in gated mode. In each pixel an

excitation gate (rectangular pulse, 20 μs long) was followed by emission collection period of ~2 ms (λ_{em}=670±35 nm). The imaging depth, excitation gate duration and laser power during the application of gate (measured after the objective) were as follows: (c) 150 μm, 20 μs, 1.32 mW; (d) 250 μm, 20 μs, 2.03mW; (e) 750 μm, 20 μs, 13.2 mW; (f) 900 μm, 50 μs, 16.3 mW.

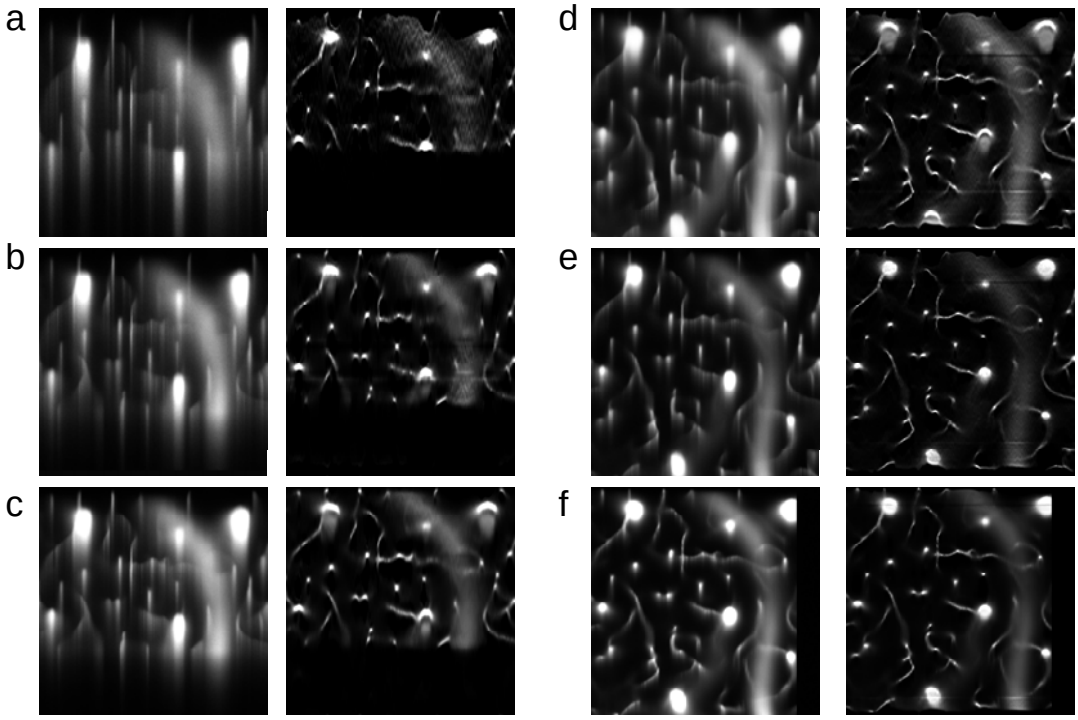

Figure S7. Images of the microvasculature at the depth of 100 μm obtained using UCNP-**11** as a marker and different scanning speeds. Left: raw image. Right: image restored by Richardson-Lucy deconvolution. Pixel dwell times: (a) 5 μs; (b) 10 μs; (c) 15 μs; (d) 20 μs; (e) 40 μs; (f) 80 μs.

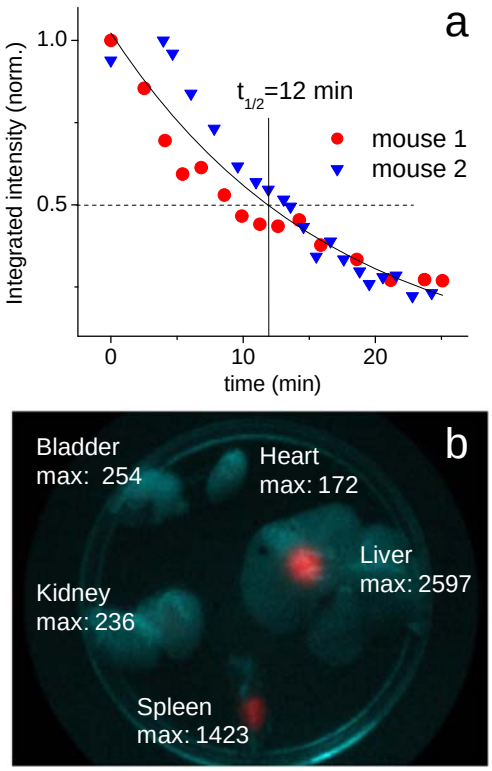

Figure S8. (a) Kinetics of clearance of UCNP-**11** from the mouse blood, measured by integrated luminescence intensity in a selected imaging plane (Z=50 μm) as a function of time. (b) Luminescence intensity in different organs was measured *ex vivo* using ICCD camera operating in D.C. mode and a laser (λ_{ex}=980nm) for excitation. The laser was coupled to a fiber and a collimator to create an excitation spot that was scanned across the organs, and the luminescence intensity was measured through a 650/40 nm band pass. The maximal attained counts are shown on the image next to each organ.

6. References

1. C. J. Hawker and J. M. J. Frechet, *J. Am. Chem. Soc.*, 1992, **114**, 8405-8413.
2. L. Twyman, A. E. Beezer and J. C. Mitchell, *Tetrahedron Lett.*, 1994, **35**, 4423-4424.
3. T. V. Esipova, X. C. Ye, J. E. Collins, S. Sakadzic, E. T. Mandeville, C. B. Murray and S. A. Vinogradov, *Proc. Natl. Acad. Sci. U. S. A.*, 2012, **109**, 20826-20831.
4. G. R. Newkome, K. K. Kotta and C. N. Moorefield, *J Org Chem*, 2005, **70**, 4893-4896.
5. A. Y. Lebedev, A. V. Cheprakov, S. Sakadzic, D. A. Boas, D. F. Wilson and S. A. Vinogradov, *ACS Appl. Materials & Interfaces*, 2009, **1**, 1292-1304.
6. T. V. Esipova, M. J. P. Barrett, E. Erlebach, A. E. Masunov, B. Weber and S. A. Vinogradov, *Cell Metab.*, 2019, **29**, 736-744.
7. T. V. Esipova, A. Karagodov, J. Miller, D. F. Wilson, T. M. Busch and S. A. Vinogradov, *Anal. Chem.*, 2011, **83**, 8756-8765.
8. M. Brettreich and A. Hirsch, *Synlett*, 1998, 1396-1398.
9. T. V. Esipova, X. Ye, J. E. Collins, S. Sakadžić, E. T. Mandeville, C. B. Murray and S. A. Vinogradov, *Proc. Natl. Acad. Sci. U.S.A.*, 2012, **109**, 20826-20831.
10. A. G. Dong, X. C. Ye, J. Chen, Y. J. Kang, T. Gordon, J. M. Kikkawa and C. B. Murray, *J. Am. Chem. Soc.*, 2011, **133**, 998-1006.
11. S. Sakadzic, E. Roussakis, M. A. Yaseen, E. T. Mandeville, V. J. Srinivasan, K. Arai, S. Ruvinskaya, A. Devor, E. H. Lo, S. A. Vinogradov and D. A. Boas, *Nat. Methods*, 2010, **7**, 755-U125.
12. M. A. Yaseen, V. J. Srinivasan, I. Gorczynska, J. G. Fujimoto, D. A. Boas and S. Sakadzic, *Biomed. Opt. Express*, 2015, **6**, 4994-5007.

7. ^{1}H and ^{13}C NMR spectra

H_2N-Glu^{1}OAll·TsOH

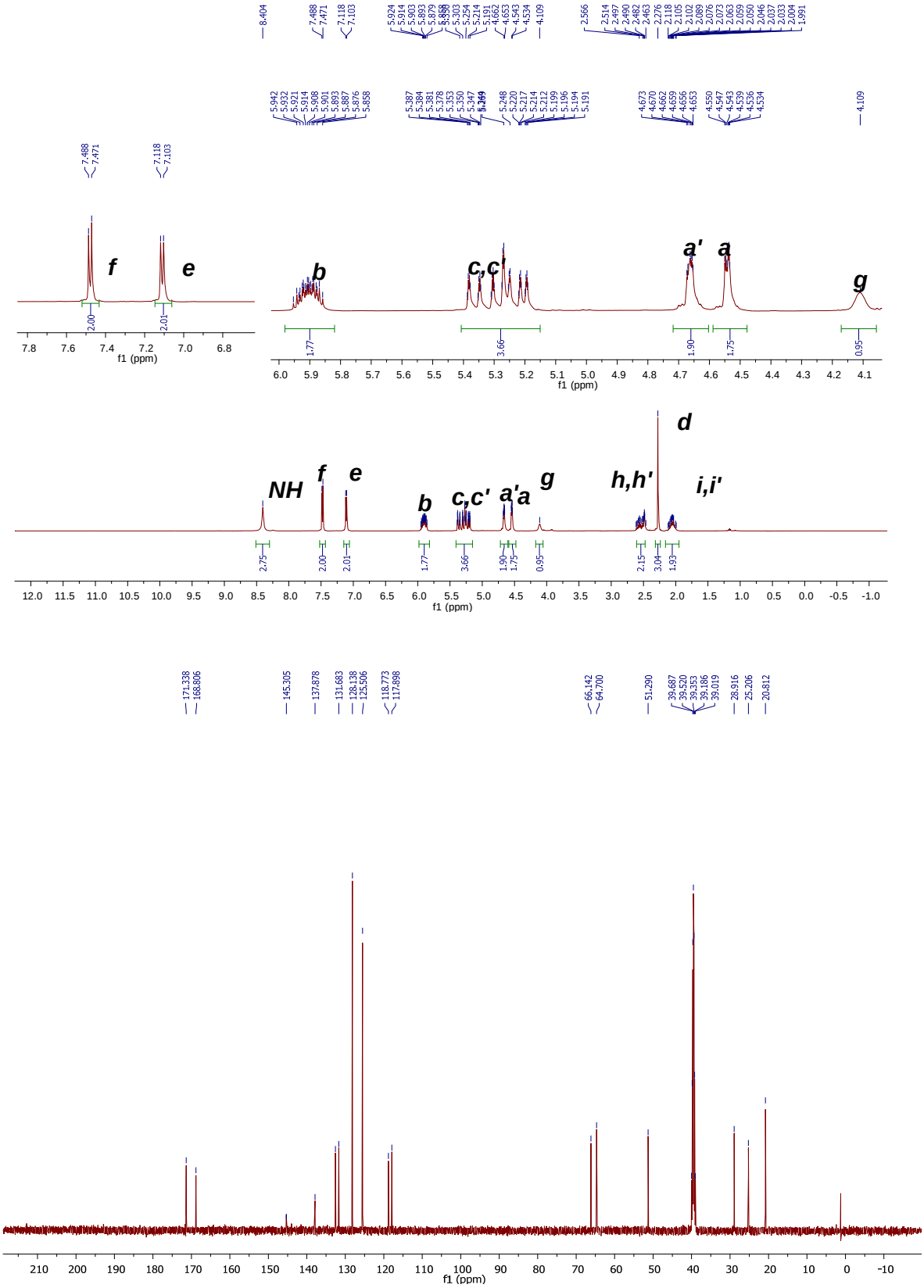

Boc-HN-Glu^{2}OAll

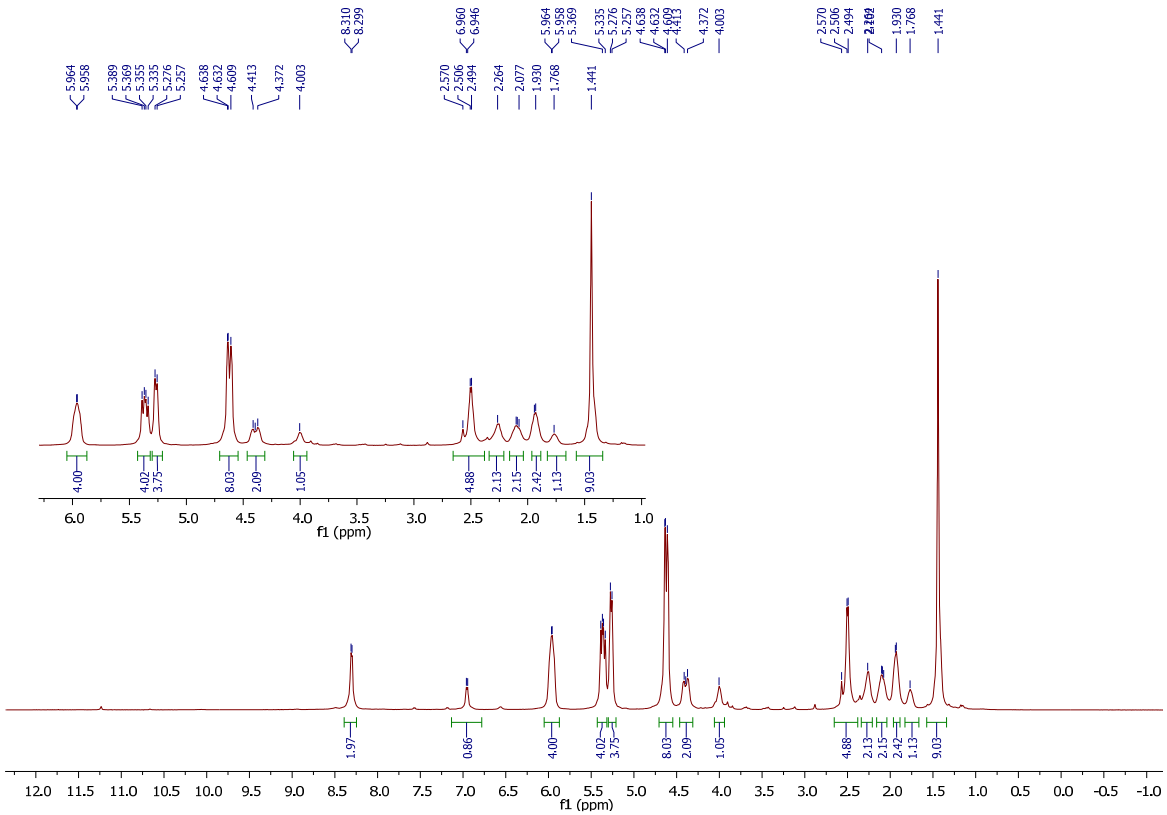

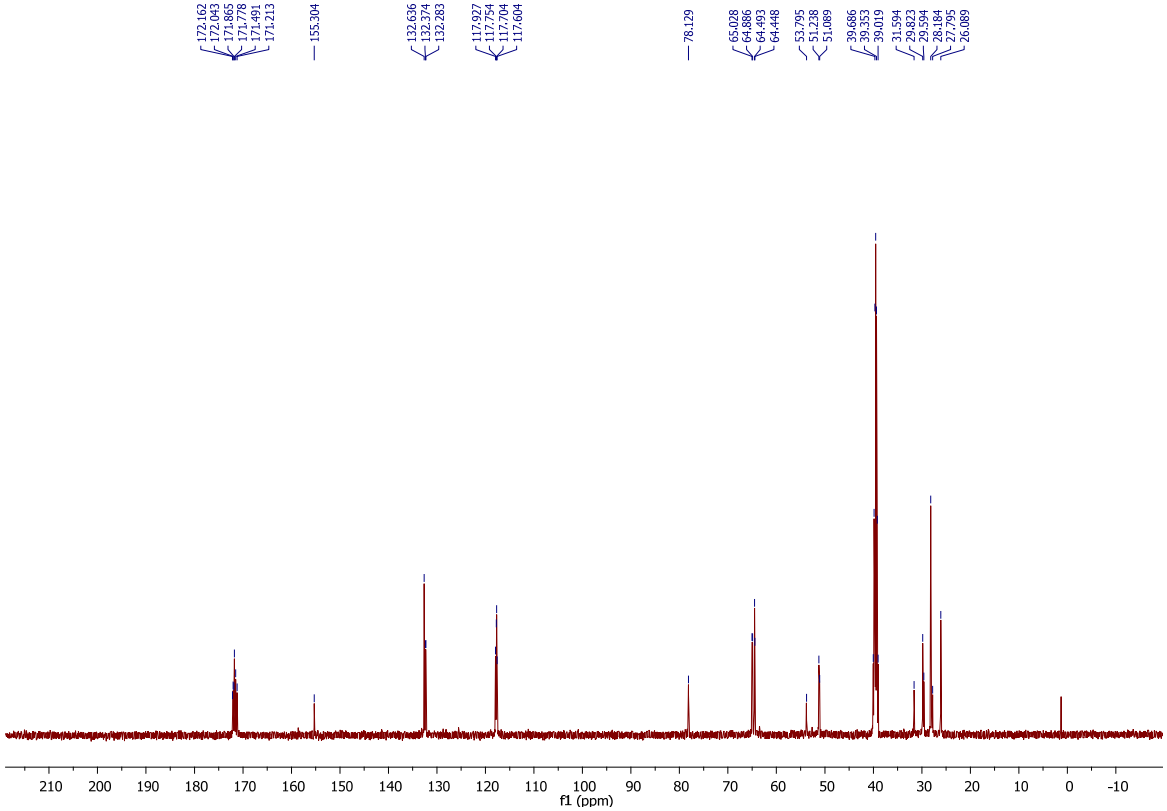

Boc-HN-Glu^{3}OAll

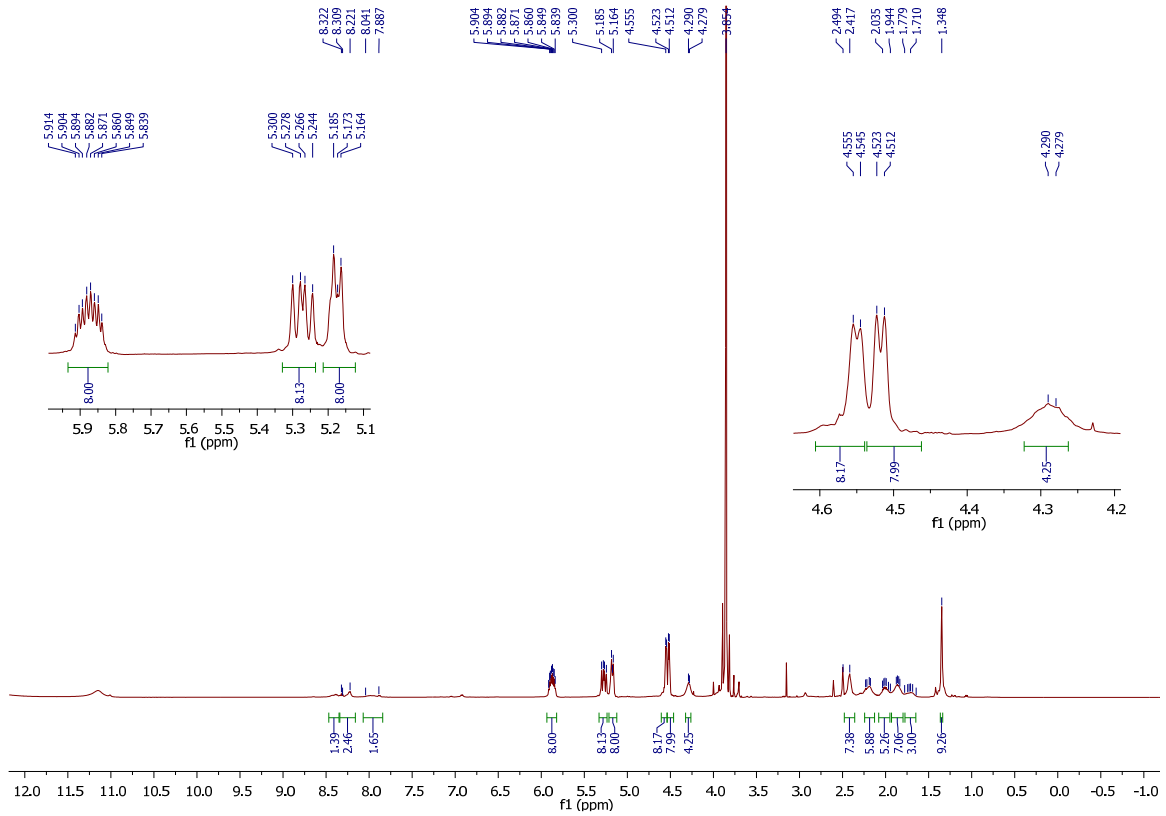

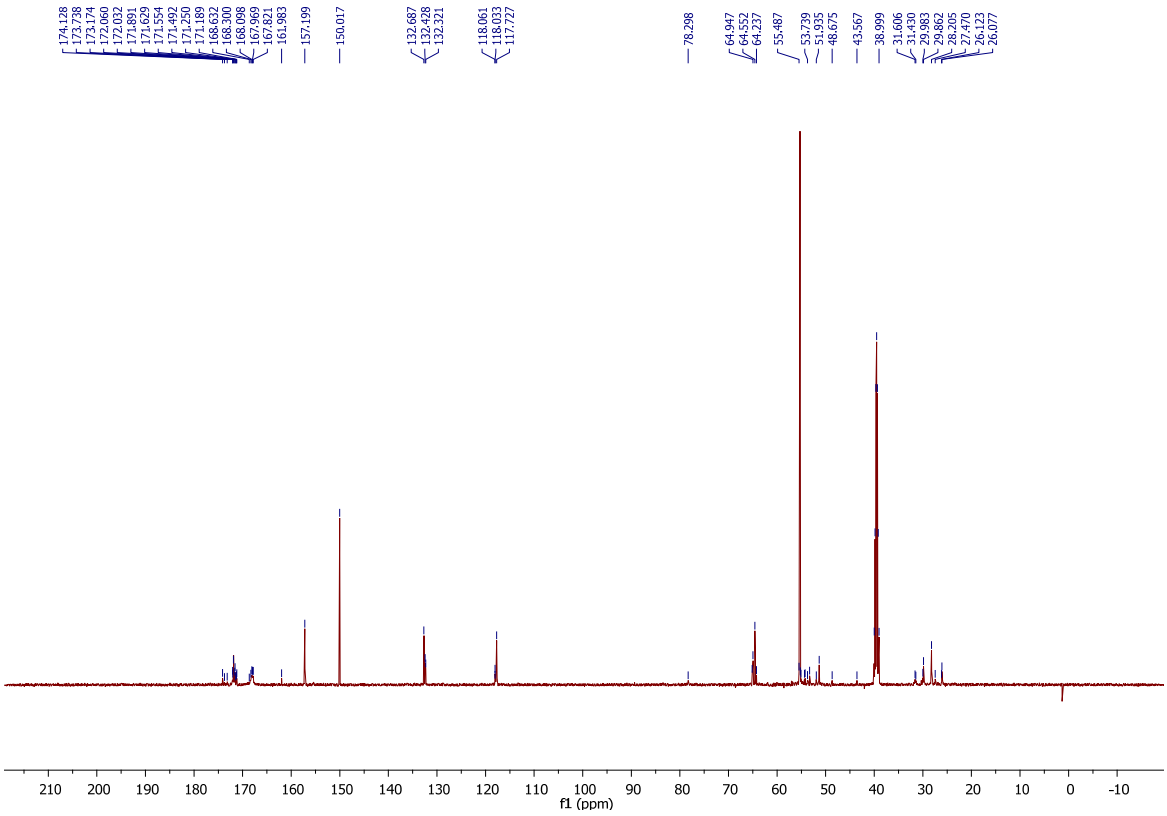

(ECR)-HN-Glu^{3}OAll (2)

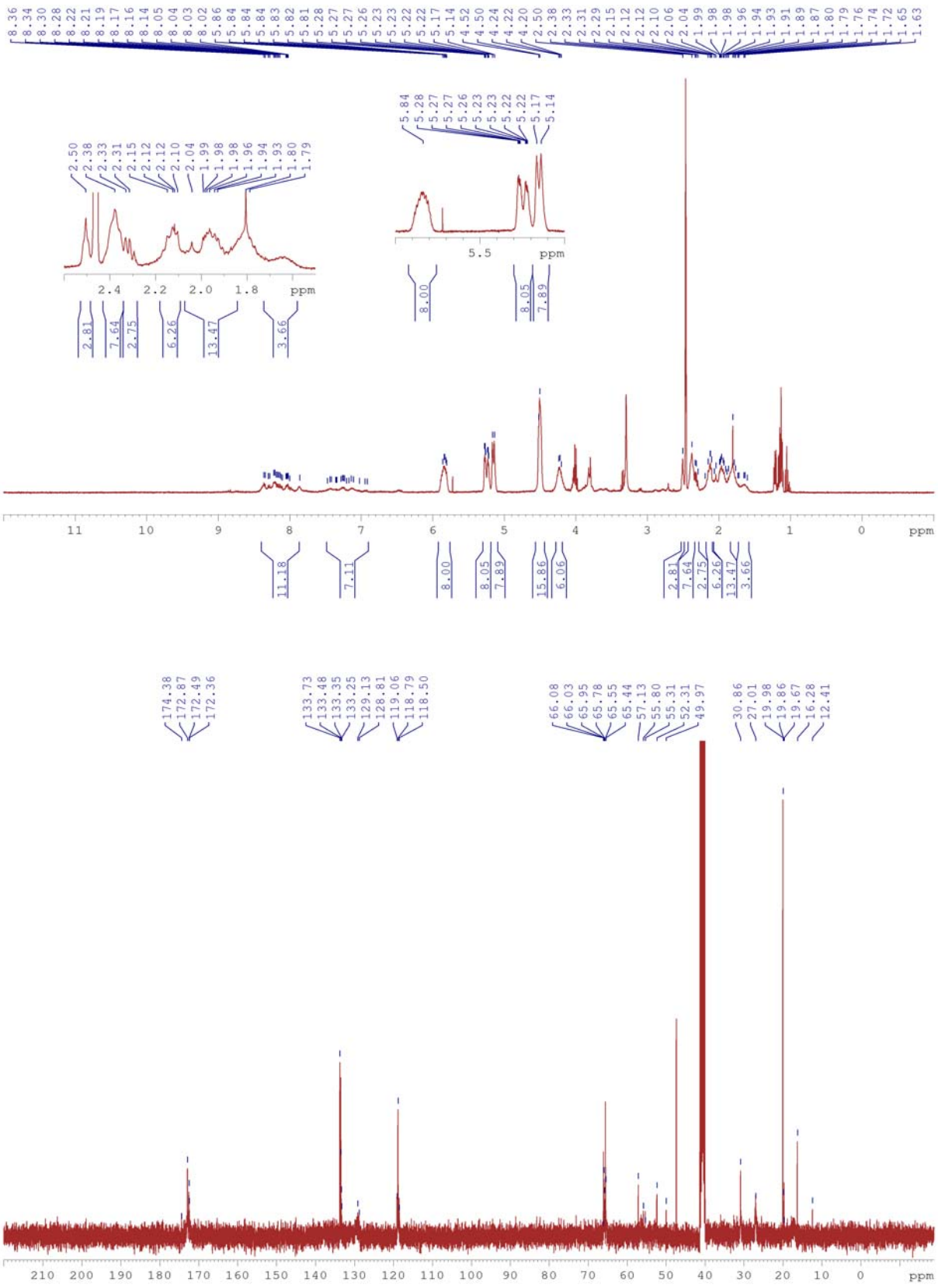

EtOGlu^{3}-NH-(ECR)-HN-Glu^{3}OAll (3)

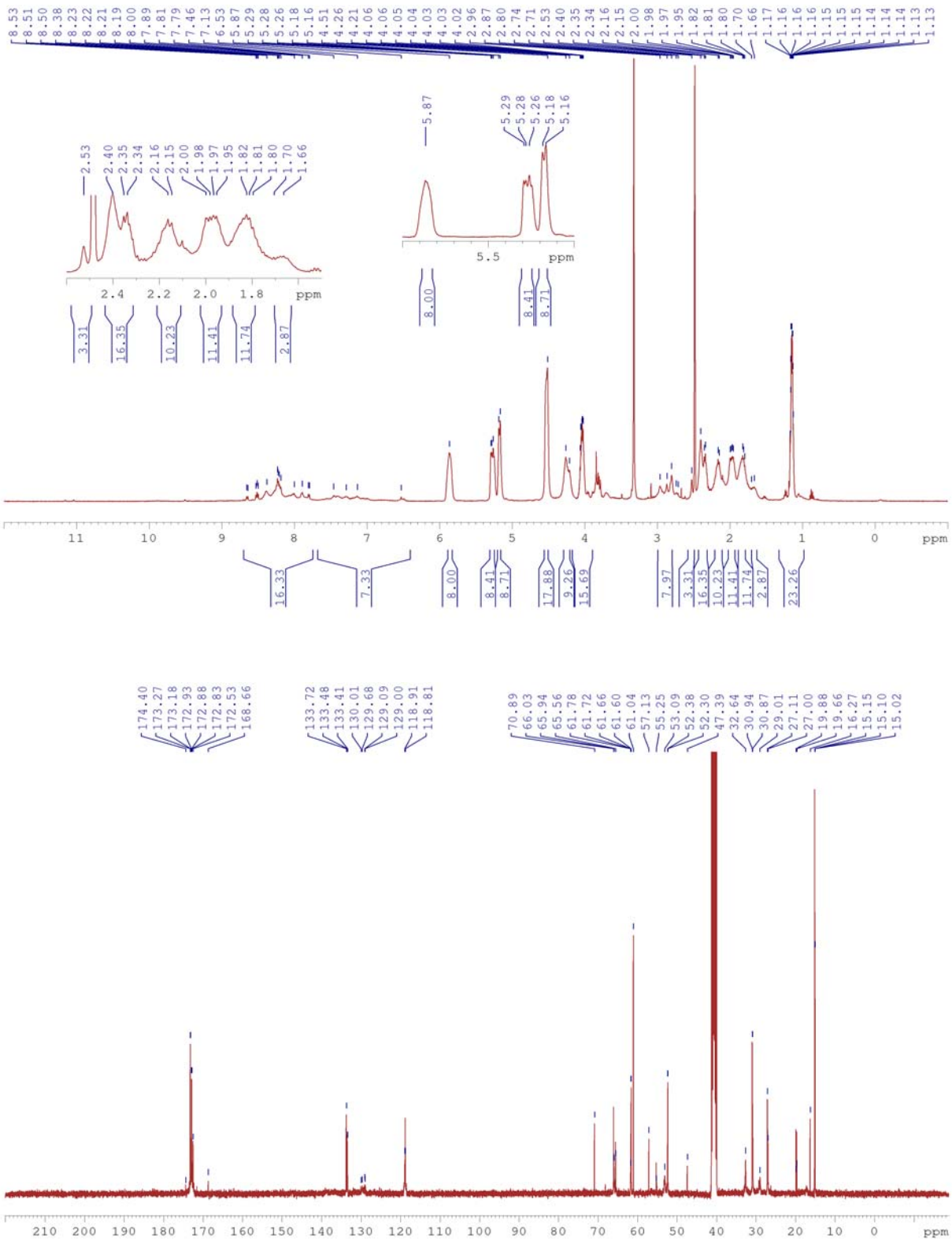

EtOGlu^{3}-NH-(ECR)-HN-Glu^{3}OH·(4)

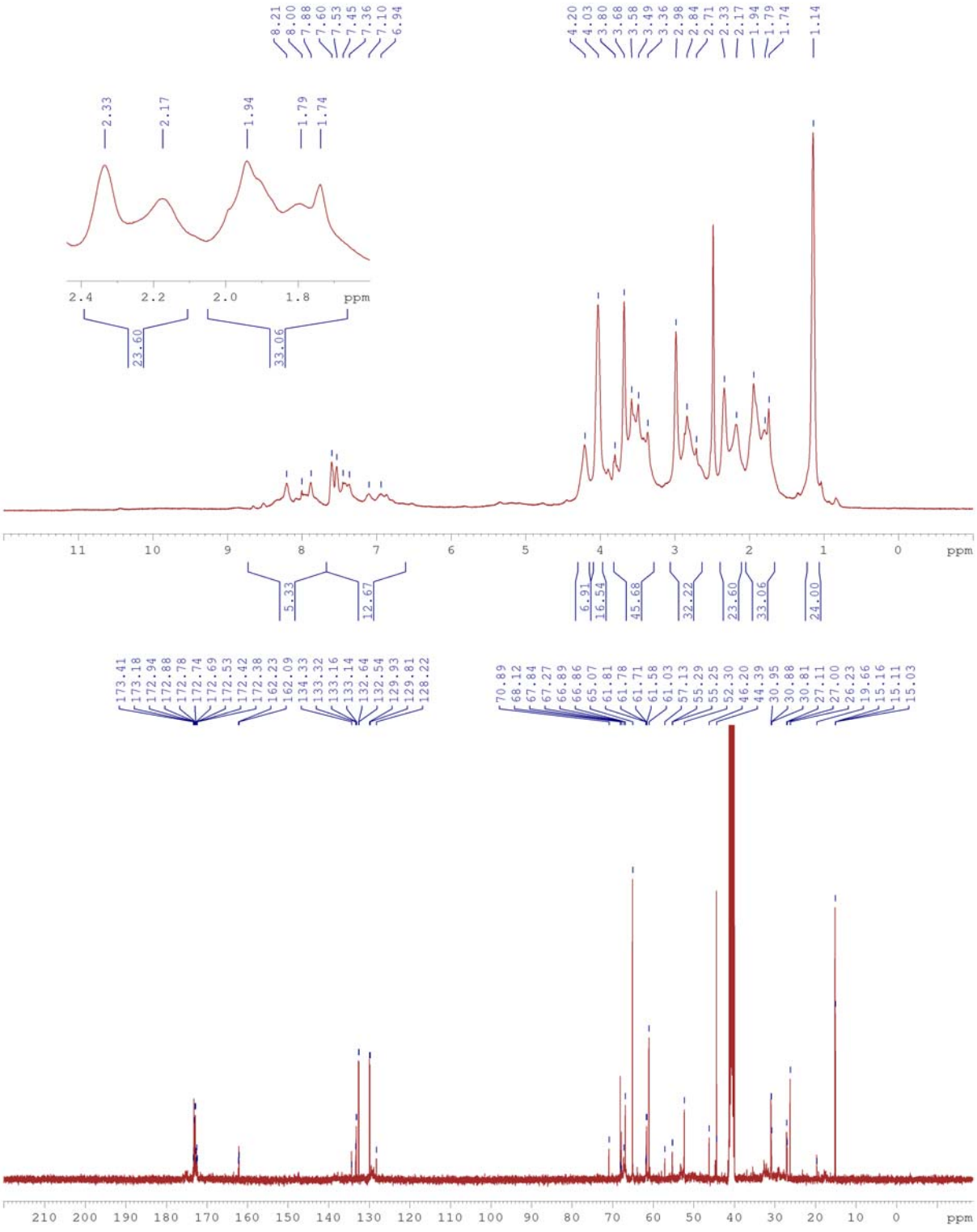

(ECR)-HN-Newk^{2}O^{t}Bu (7)

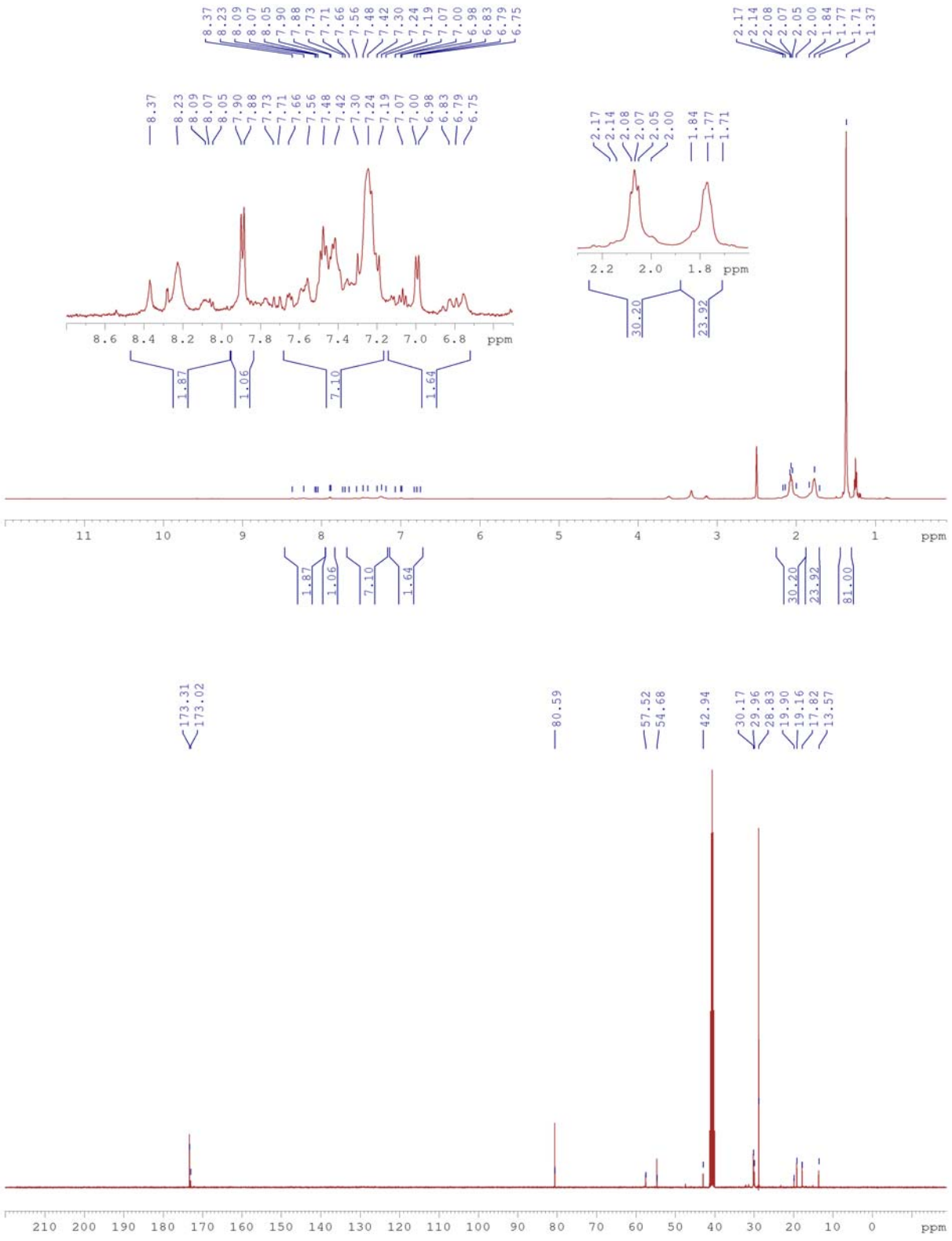

EtOGlu^{3}-NH-(ECR)-HN-Newk^{2}O^{t}Bu (8)

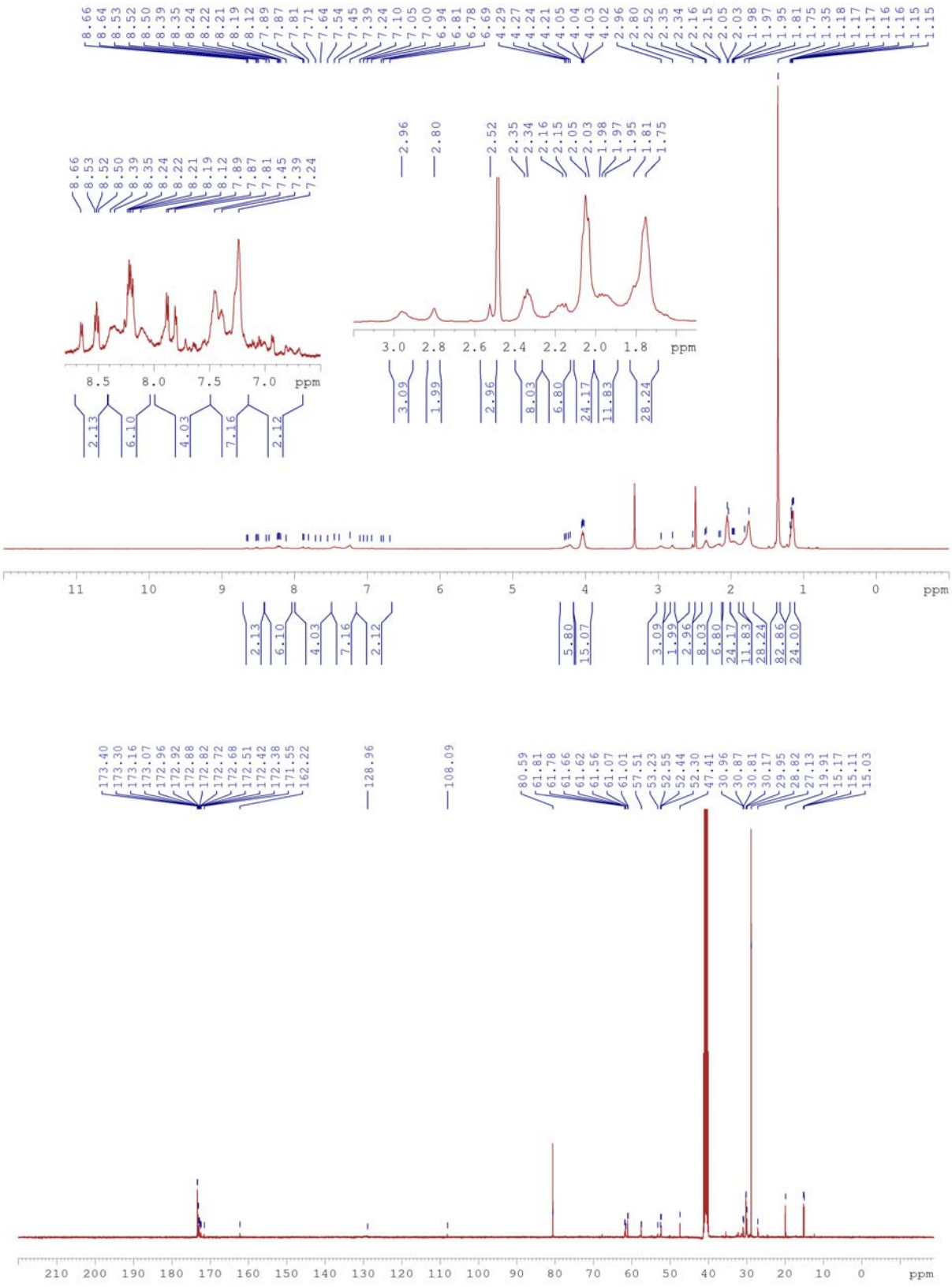

EtOGlu^{3}-NH-(ECR)-HN-Newk^{2}OH (9)